

HIGHWAY RESEARCH RECORD

Number 192

Cement
Hydration

3 Reports

Subject Area

32 Cement and Concrete

HIGHWAY RESEARCH BOARD

DIVISION OF ENGINEERING NATIONAL RESEARCH COUNCIL
NATIONAL ACADEMY OF SCIENCES—NATIONAL ACADEMY OF ENGINEERING

Washington, D.C., 1967

Publication 1523

Price: \$1.50

Available from

Highway Research Board
National Academy of Sciences
2101 Constitution Avenue
Washington, D.C. 20418

Department of Materials and Construction

R. L. Peyton, Chairman
Assistant State Highway Engineer
State Highway Commission of Kansas, Topeka

HIGHWAY RESEARCH BOARD STAFF

R. E. Bollen, Engineer of Materials and Construction
W. G. Gunderman, Assistant Engineer of Materials and Construction

CONCRETE DIVISION

Bryant Mather, Chairman
Chief, Concrete Division, Waterways Experiment Station
Jackson, Mississippi

COMMITTEE ON BASIC RESEARCH PERTAINING TO PORTLAND CEMENT AND CONCRETE

(As of December 31, 1966)

W. L. Dolch, Chairman
Joint Highway Research Project, Purdue University
Lafayette, Indiana

- H. A. Berman, Heat Measurements Section, National Bureau of Standards, Washington, D.C.
- Stephen Brunauer, Chemistry Department, Clarkson College, Potsdam, N. Y.
- L. E. Copeland, Portland Cement Association, Skokie, Illinois
- Sidney Diamond, Associate Professor of Engineering Materials, Civil Engineering School, Purdue University, Lafayette, Indiana
- Wilhelm Eitel, The University of Toledo, Toledo, Ohio
- G. J. C. Frohnsdorff, American Cement Corporation, Riverside, California
- Kenneth T. Greene, Research Petrographer, Ideal Cement Company, Fort Collins, Colorado
- P. E. Halstead, Cement and Concrete Association, Wexham Springs, Framewood Road, Stoke Poges, Slough, Bucks., England
- R. L. Handy, Civil Engineering Department, Iowa State University, Ames
- W. C. Hansen, Consulting Chemist, Valparaiso, Indiana
- George L. Kalousek, Research Advisor—Concrete, U. S. Bureau of Reclamation, Denver, Colorado
- Clyde E. Kesler, Department of Theoretical and Applied Mechanics, University of Illinois, Urbana
- Alexander Klein, Lecturer in Civil Engineering, University of California, Berkeley
- K. R. Lauer, Associate Professor of Civil Engineering, University of Notre Dame, Notre Dame, Indiana
- Katharine Mather, Waterways Experiment Station, Jackson, Mississippi
- Richard C. Mielenz, Vice President for Product Development, The Master Builders Company, Cleveland, Ohio
- R. E. Philleo, Department of the Army, Office, Chief of Engineers, Civil Works Engineering Division, Concrete Branch, Washington, D.C.
- T. C. Powers, Barrington, Illinois
- Mrs. Della M. Roy, Materials Research Laboratory, The Pennsylvania State University, University Park
- Peter J. Sereida, National Research Council, Ottawa, Ontario, Canada
- E. G. Swenson, Inorganic Materials Section, Division of Building Research, National Research Council of Canada, Ottawa, Ontario, Canada
- H. F. W. Taylor, Department of Chemistry, University of Aberdeen, Old Aberdeen, Scotland
- Rudolph C. Valore, Valore Research Associates, Ridgewood, New Jersey
- George J. Verbeck, Director of Research, Portland Cement Association, Skokie, Illinois

Foreword

The three papers in this RECORD concern the processes and reactions that take place in hydrating portland cements. They should be of interest to those concerned with the chemical reactions in such systems and with the strength developed in the resulting binder.

Mehta and Klein examined cements in which the aluminum was either in the form of the small amount in the alite phase or combined with iron in various ferrite compositions. They examined the pastes for the presence of ettringite, calcium aluminate trisulfate hydrate, and for the monosulfate form, by X-ray diffraction, and delineated the conditions under which these compounds form in such systems.

Srinivasan examined the reactions of various forms of silica and lime in aqueous systems. The silica was heated to produce various degrees of crystallinity and the differences in the reactivity of these various forms were studied. The chemical processes in such reactions are discussed and their possible relationships to the strength produced, which have obvious implications in pozzolanic systems, were examined.

Popovics's paper is an interesting attempt to determine a "model" for a hydrating portland cement. His model is a mathematical one that assumes a two-component mixture—the tricalcium silicate and everything else. The model also assumes that the deceleration in strength development of either component is proportional to the strength it has reached at a given time. On the basis of these and other assumptions an equation was derived by means of which the strength at later ages can be predicted from early behavior. A large amount of experimental data of other workers was then examined in order to test the validity of the model and resulting prediction equation.

—W. L. Dolch

Contents

✓ A	INFLUENCE OF THE STRUCTURAL STATE OF SILICA ON LIME-SILICA REACTIONS	
	N. R. Srinivasan	1
	A MODEL FOR THE KINETICS OF THE HARDENING OF PORTLAND CEMENT	
	Sandor Popovics	14
✓ A	FORMATION OF ETTRINGITE IN PASTES CONTAINING CALCIUM ALUMINOFERRITES AND GYPSUM	
	P. K. Mehta and A. Klein	36

Influence of the Structural State of Silica on Lime-Silica Reactions

N. R. SRINIVASAN, Central Road Research Institute, New Delhi

The reactions in lime-silica pastes showing pozzolanic action and certain aspects of cement hydration were studied, employing silica samples of different crystallographic characteristics. It is shown that the structural state of these samples greatly influences the reactions. The nature of the reaction products and the mode of their formation were also studied through chemical analysis and X-ray and electron microscope studies. The results are discussed and tentative conclusions are given.

•THE CaO - SiO₂ - H₂O system has been investigated by many researchers who have regarded it as the fundamental basis for understanding cementitious reactions. However, almost all the investigations conducted at temperatures below 100 C were carried out in the presence of excess water. Investigations on lime-silica pastes are rare mainly because the attainment of equilibrium is difficult and may require a long period of time. However, the lime-silica paste reactions resemble cement reactions under actual conditions, and even if metastable compounds were to form, these would occur under practical as well as laboratory conditions, affecting the various characteristics of the hardening mass. With this in view, a series of investigations was undertaken at the Central Road Research Institute, New Delhi, on different pastes involving lime, silica, alumina and iron oxides. The present paper describes the investigations on lime-silica paste. It gives an account of the various silica gels used in the study and of the lime-silica reactions.

EXPERIMENTAL APPROACH

Materials and Methods of Preparation

Details regarding the six different silicas used in this study are given in Table 1.

The lime used in preparing the micro-cube specimens for strength tests was chemically pure calcium hydroxide from the British Drug House. For the preparations of pastes for chemical analysis and X-ray and electron micrograph studies, fresh lime prepared by calcining precipitated calcium carbonate at 1000 C was used.

Pattern of Investigation

The broad classifications of the experiments conducted are as follows.

1. A general study of the physical properties of the silica samples.
2. Determination of the pozzolanic reactivities of the calcined silica samples by means of a micro-cube method.
3. Study of the reaction products of pozzolanic reaction.

A few experiments to evaluate the effects of using partially carbonated lime on the strength development characteristics of lime-silica paste were also included.

TABLE 1
DETAILS OF SILICA SAMPLES

Designation of Silica Gels	Description	Source
S-1	Silica gel for partition chromatography, granular and uniform sized	E. Merck
S-3	Silica precipitated, light, fluffy and fine powder	British Drug House
S-4	Silica dehydrant, white or light brown, angular aggregate pieces about $\frac{3}{16}$ in. and less	
S-5	Silica, white, chalky precipitate	Laboratory preparation ^a
S-6	Silica gel, white, gelatinous	Laboratory preparation ^b
S-7	Silica gel, white	Laboratory preparation ^c

^aTo 200 cc of a 37.7 percent solution of sodium silicate (analysis of sodium silicate: SiO₂ - 24 percent; Na₂O - 11.6 percent loss on drying - 64.4 percent), concentrated hydrochloric acid was added little by little while stirring and diluting the mixture, keeping the pH below 2. The white, chalky precipitate obtained was filtered and washed with hot distilled water several times. The silica was dried at 110 C and kept in glass stoppered bottles. It had a loss on ignition of 11.5 percent and a Cl-0.017 percent.

^bTo 1000 cc of a 20 percent solution of commercial sodium silicate of the mentioned composition, 1610 cc of 5 percent hydrochloric acid was slowly added with adequate stirring. The final pH was between 8 and 9. Gelation occurred in a few minutes. The gel was aged overnight, broken, washed with hot water, filtered, dried and stored. It had a loss on ignition of 8.5 percent and a Cl content of 0.012 percent.

^cTo 2000 cc of a 5 percent hydrochloric acid solution, 1140 cc of 20 percent solution of the commercial sodium silicate was added. The final pH was 4.0. Gelation was slow. The finally washed and dried sample had a loss on ignition of 13.5 percent and a chloride content 0.015 percent.

TABLE 2
SPECIFIC GRAVITY OF SILICA SAMPLES

Sample Number	Specific Gravity			
	Raw	600 C	800 C	1000 C
S-1	2.11	2.09	2.24	2.26
S-3	1.94	1.95	2.04	2.21
S-4	1.74	1.94	1.94	2.09

TABLE 3
SURFACE AREA OF SILICA BY METHYL RED ADSORPTION

Sample Number	Surface Area (m ² /gm)			
	Raw	600 C	800 C	1000 C
S-1	50.2	50.3	56.5	45.3
S-3	84.8	71.5	63.0	59.7
S-4	N.D.	60.0	46.7	51.4
S-5	75.8	78.1	61.6	50.5
S-7	59.8	71.2	N.D.	75.7

TABLE 4
BOUND WATER CONTENTS AND CALCULATED FORMULAS FOR SILICA SAMPLES

Sample Number	Bound Water (%)			Calculated Formulas		
	Raw	600 C	800 C	Raw	600 C	800 C
S-1	4.0	1.0	0.3	S ₂₇₆ H ₄₀	S ₂₃₇ H ₁₀	S ₂₅₆ H ₃
S-3	5.0	1.0	0.5	S ₂₈₅ H ₅₀	S ₂₃₇ H ₁₀	S ₂₅₆ H ₅
S-4	11.5	1.0	0.3	S ₂₆₀ H ₁₁₅	S ₂₃₇ H ₁₀	S ₂₅₆ H ₃
S-5	8.5	2.0	1.0	S ₂₇₅ H ₂₅	S ₂₅₄ H ₂₀	S ₂₃₇ H ₁₃
S-7	13.5	7.5	4.5	S ₂₆₀ H ₁₃₅	S ₂₄₁ H ₇₅	S ₂₃₇ H ₄₅

Physical and Chemical Properties of Silicas Used

Specific Gravity—The specific gravities of raw silicas S-1, S-3 and S-4 and of the calcined samples derived from these silicas were determined on the powdered samples passing B.S. 100 sieve by the usual specific gravity bottle method, using redistilled kerosene as the liquid medium. The calcined samples for this and all subsequent experiments were prepared by calcining about 100 gm of the raw samples in fused silica dishes, using an electric muffle furnace at the specified temperature for a minimum period of 3 hours, after which the furnace was turned off. The samples were allowed to cool in the furnace overnight and were then ground to a fineness of -100 B.S. sieve. The specific gravity results are given in Table 2.

Hydroxylated Surface Area—The surface area of the various silica samples was determined by the methyl red adsorption method described by Shapiro and Kolthoff (1), using a Hilger's Spekkar absorptiometer with 5750 Å filter to measure the amount of dye absorbed (Table 3).

Dehydration Studies—The loss of weight suffered by the silica after dehydration at different temperatures was determined for

the silica samples S-1, S-3, S-4, S-5, and S-7. From these values, the amount of "bound water" after calcination at different temperatures was calculated. In the case of the raw samples, the loss between 115 C and 1000 C was taken to be the bound water (Table 4).

Particle Size—The calculated formulas from the dehydration data (Table 4) were used in Pier's derivations (2) for x and y in the general formulas S_xH_y derived from Carman's concept of colloidal silica particles (3).

$$x = \frac{22}{6} \pi d^3 \quad (1)$$

$$y = \frac{\pi}{2} (2.8 d)^2 \quad (2)$$

Dividing Eq. 1 by Eq. 2,

$$\frac{x}{y} = 0.931 d \quad (3)$$

where d is the particle diameter in millimicrons.

Using Eq. 3, the particle size in millimicrons calculated for the ultimate particles of silicas from the dehydration data is obtained (Table 5).

X-ray Studies—X-ray patterns were taken, using copper radiation for samples S-1, S-3 and S-4 after calcination at 800 C and 1000 C. Patterns for these samples calcined at temperatures below 800 C were not taken because no crystallographic changes were expected for the silica gels below this temperature. In the case of S-5, X-ray patterns were taken after calcination at 600 C and 1000 C (Fig. 1).

The first three samples after calcination at 800 C still showed the usual pattern for silica gels, with a broad band in the region of 3.9 to 4.7 Å. After calcination at 1000 C, S-1 maintained this strong band, but a strong line at 4.19 Å was visible in the band. Another strong line at 3.32 Å also occurred. The two strong lines revealed the crystallization of quartz from the silica samples. After calcination at 1000 C, sample S-3 showed considerable

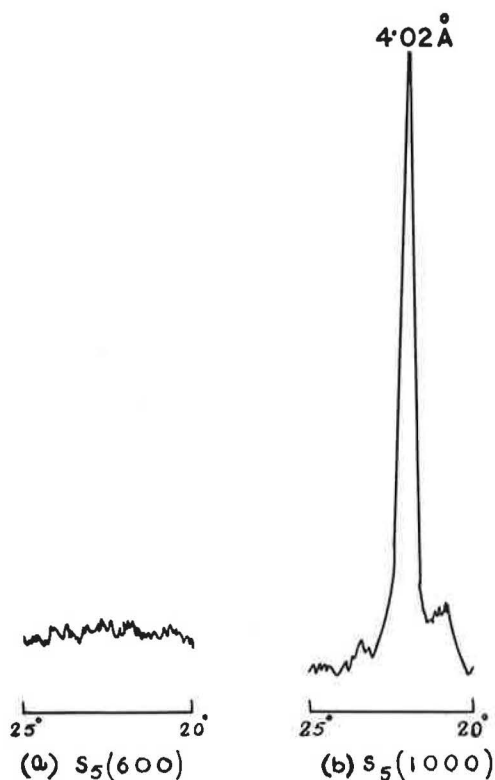


Figure 1. X-ray diffractometer patterns for S-5 (600 C) and S-5 (1000 C).

TABLE 5
COMPUTED SIZE OF ULTIMATE
PARTICLES OF SILICAS

Sample Number	Particle Size in Millimicrons		
	Raw	600 C	800 C
S-1	7.5	32	107
S-3	6.1	32	64
S-4	2.5	32	107
S-5	3.5	16	25
S-7	2.1	3.6	6.9

weakening of the 3.9 to 4.7-Å band, and the emergence of a line at 4.01 Å revealed the conversion of the silica to cristobalite. No quartz lines were visible. Similarly, S-4 calcined at 1000 C showed a strong cristobalite line at 4.01 Å in the 3.9 to 4.7-Å band.

Determination of Pozzolanic Activity—The following accelerated strength test to measure the pozzolanic activity of raw and calcined samples of silica was used in this study.

Three grams of calcium hydroxide (British Drug House) were mixed with 6 gm of the silica powder, and a predetermined amount of water (Table 6) was added to form a dry consistency paste. The water addition was determined by a micro-consistometer (Fig. 2). It was specified that the needle should penetrate 2 to 4 mm from the surface of a

TABLE 6
COMPRESSIVE STRENGTH DEVELOPED BY
SILICA-LIME PASTES

Sample Number	Micro-Cube Strength (psi) ²					
	W/S	600 C	W/S	800 C	W/S	1000 C
S-1	0.83	706	0.92	640	0.20	2253
S-3	1.50	2160	1.67	1200	0.83	2213
S-4	0.50	800	0.42	726	0.42	1293
S-5	0.94	2540	N.D.	N.D.	0.62	812
S-6	1.09	1980	N.D.	N.D.	0.41	284
S-7	0.88	1940	N.D.	N.D.	0.33	2252

²Average of 3 cubes.

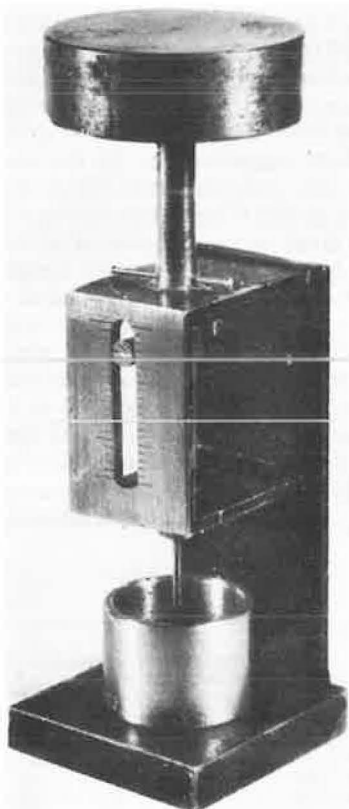


Figure 2. Micro-consistometer.

pat of paste at the right consistency. Three 1/2-in. cubes were cast, using this paste. These were cured in the mold for 24 hr under humid conditions, after which they were cured for a further period of 48 hr at 50 C and 100 percent humidity. At the end of the period, the cubes were removed and tested for compressive strength.

The strength developed is taken as an index of pozzolanic activity. It is considered "medium active" if the strength is 800 to 1000 psi, "reactive" if it is 1000 to 1500 psi, and "very reactive" if above 1500 psi. The results of micro-cube tests are given in Table 6.

In the case of the finely divided S-3 sample, the following additional factors were studied: (a) the effect of polymerization of silica on strength development, and (b) the effect of admixture of hard quartz particles on the strength development of silica pastes.

The evaluation of the effects of using partially carbonated lime on the strength development characteristics was also included in this group of sub-experiments.

To study the effect of polymerization of silica on strength development, a paste was made of S-3 raw silica alone without the addition of lime, and the micro-cube strength was determined in the usual manner using this paste. To study the effect of hard, inert materials on the strength development of silica paste, the S-3 raw sample was mixed with quartz powder passing B.S. 100 sieve in the ratio, silica: sand = 2:1 by weight, and the paste made with this mixture without the addition of lime was used to determine micro-cube strength in the usual way. To determine the effect of carbonation of lime, different proportions of calcium carbonate were mixed with the lime normally used for the micro-cube tests (Table 7) to yield carbonated limes, and these were used for the normal micro-cube test.

An attempt was also made to relate the percentage of cementitious compounds

TABLE 7
COMPRESSIVE STRENGTHS OF SILICA PASTES
AND CARBONATED LIME-SILICA PASTES

Composition of Micro-Cubes	Micro-Cube Strength (psi)
S-3 paste without lime	320
S-3 plus quartz powder without lime	1,468
S-3 with lime carbonated to 20 percent	1,868
S-3 with lime carbonated to 30 percent	1,500
S-3 with lime carbonated to 50 percent	1,001
S-3 with 100 percent CaCO ₃	136

TABLE 8
SILICA SOLUBILITY BY HCl TREATMENT OF LIME-SILICA
PASTES AND THEIR MICRO-CUBE STRENGTHS

Lime-Silica Paste	Percent Soluble Silica In:		Micro-Cube Strength (psi)
	Paste	Silica	
S-1 600 C	1.00	Nil	706
S-1 800 C	0.8	Nil	640
S-1 1000 C	5.0	Nil	2253
S-3 600 C	2.0	Nil	2160
S-3 800 C	2.6	Nil	1200
S-3 1000 C	5.5	Nil	2213
S-4 600 C	5.0 to 6.0	Nil	800
S-4 800 C	5.0 to 6.2	Nil	726
S-4 1000 C	6.2 to 7.2	Nil	1293
S-5 600 C	4.4	Nil	2540
S-5 1000 C	2.7	Nil	812
S-6 600 C	4.1	Nil	1980
S-6 1000 C	1.5	Nil	284
S-7 600 C	4.1	0.1	1940
S-7 1000 C	0.9	0.1	2252

method (ASTM C-25-44) because this was felt to be better suited for the lime rich lime-silica pastes which did not contain any hard-burnt calcium oxide which may call for a more drastic treatment such as ethylene glycol extraction. Total lime and soluble silica in the pastes were determined from the acid extracts of these pastes using 1:3 HCl. The reasons for deleting the alkali extraction procedure after acid treatment were mentioned previously. The extracts were analyzed for silica and calcium oxide by the methods used for portland cement analysis.

To calculate the calcium oxide in the cementing phase, the sum of the CaO present as CaCO₃ and available lime was deducted from the total CaO percent. This CaO was assumed to be combined with the determined soluble silica for calculating the composition of the cementing phase. The validity of this assumption and the extent of accuracy of the calculated compositions are discussed in detail separately. At this stage it may be enough to state that the compositions given in Table 9 for the cementing phase can only be considered approximate.

The results in Table 9 include those for the following investigations: (a) the effect of calcination of silica on the composition of the cementing phase, (b) the effect of curing temperature of the pastes on the composition of the cementing phase, (c) the effect of the initial CaO:SiO₂ ratio of the paste on the final composition of the cementing phase, and (d) the effect of initial consistency of pastes on the composition of the cementing phase.

X-ray Studies—The X-ray diffraction patterns were made of aged lime-silica pastes prepared from lime and the following silica gels: S-3 raw, S-3 (1000 C), S-4 (600 C), S-4 (1000 C), S-5 (600 C), and S-5 (1000 C).

Copper radiation was used. The pastes were kept in sealed glass vials for a year before the patterns were taken. Figure 3 shows the results obtained for S-5 (600 C) and S-5 (1000 C) pastes.

formed through the estimation of silica made soluble through interaction with lime in a 1:3 hydrochloric acid solution, after testing some of the micro-cubes. A procedure which avoids extraction with sodium hydroxide or sodium carbonate was deliberately adopted to prevent the errors resulting from the passing into such alkaline solutions of unreacted silica in the lime-silica gel pastes, which would give misleading figures of soluble silica. The procedure adopted was in line with that adopted by Steope (4). Table 8 gives the results of acid extraction as related to micro-cube strengths.

Study of Reaction Products in CaO - SiO₂ - H₂O System

Chemical Analysis—Lime-silica pastes kept in a sealed glass vial for about one year or more were chemically analyzed by standard methods. The loss of weight at 115 C was taken to be due to loss of free water. The loss on ignition at 1000 C represented the loss due to free water, carbon dioxide and structural water. All the carbon dioxide that was determined was assigned to calcium carbonate which was thus estimated. The available lime, representing the unreacted lime as calcium hydroxide, was determined by the sugar

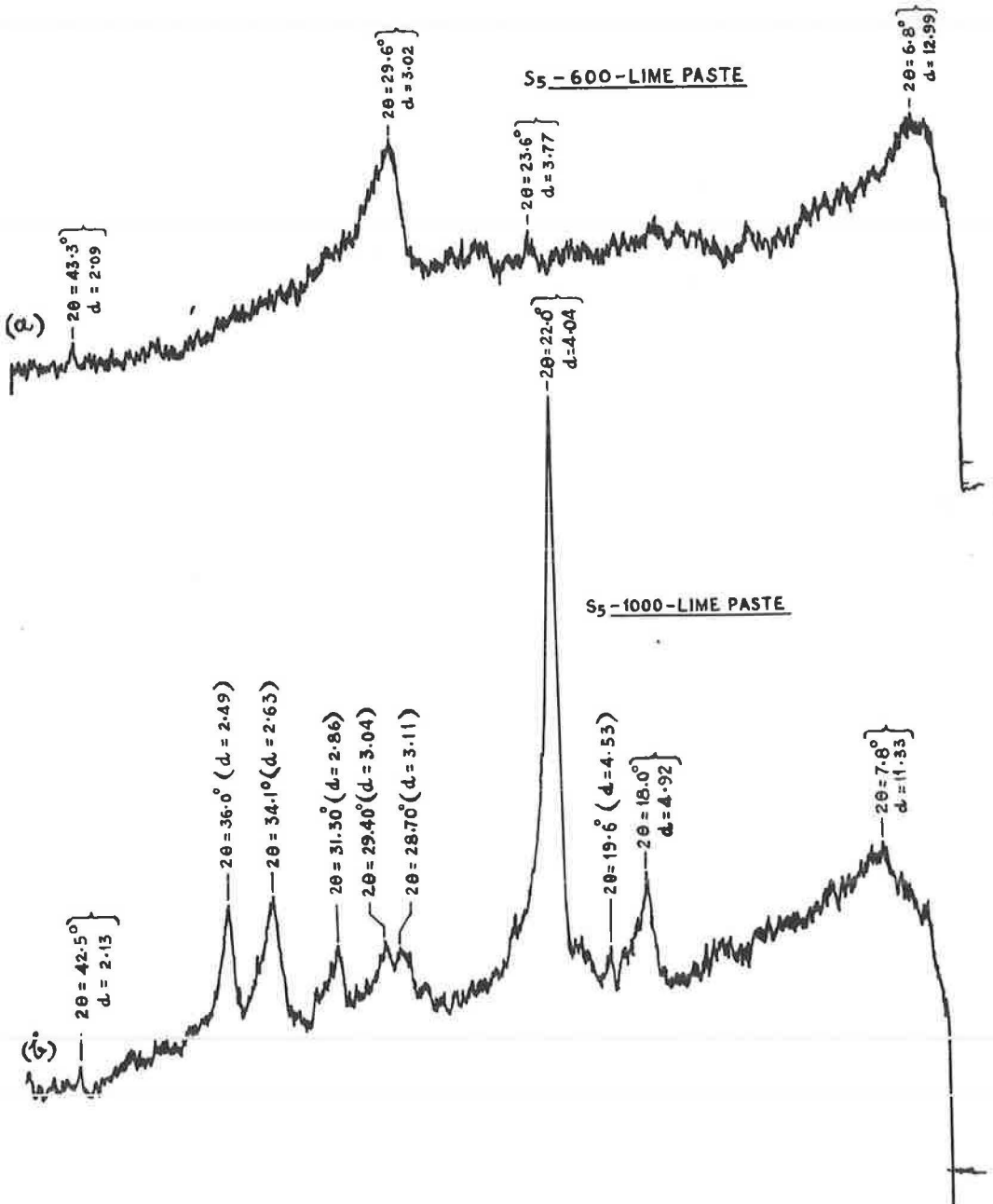


Figure 3. X-ray diffraction chart tracings for lime-silica pastes.

Electron Micrograph Studies—Several electron micrographs of the lime-silica reacted products were taken with a RCA electron microscope. The pastes used were made with freshly prepared lime and the following silica gels: S-3 raw, S-3 (1000 C), and S-4 (1000 C). A small quantity of the hardened paste was powdered and dispersed in water and examined at a magnification of about 21,000.

Dehydration of Lime-Silica Paste—A lime-silica paste made with freshly prepared lime and S-3 raw was dehydrated in a Stanton thermobalance with a heating rate of about

TABLE 9
ANALYSIS OF LIME-SILICA PASTES PREPARED FROM S-3 AND S-4 SAMPLES

Description of Paste	CaO Phase (%)				Soluble SiO ₂ (%)	Water Phase					Apparent Comp. of Cementing Phase
	Total CaO	CaO in Ca(OH) ₂	CaO in CaCO ₃	CaO in Cementing Phase		Loss on Ignition	Loss Due to Ca(OH) ₂	Loss Due to CaCO ₃	Loss Due to Free Water	Water in Cementing Phase	
(a) Effect of calcination of silica on the composition of the paste (paste composition CaO:SiO ₂ = 1:2 ordinary curing)											
CaO + S ₄ 600	21.52	4.40	6.35	10.77	4.98	35.9	1.47	5.0	26.2	3.73	C _{2.3} SH _{1.78}
CaO + S ₄ 800	20.46	11.80	3.30	5.36	5.08	24.2	3.93	2.6	13.4	4.30	C _{1.1} SH _{1.78}
CaO + S ₄ 1000	22.2	10.60	3.40	8.20	6.16	27.3	3.53	3.4	19.0	1.40	C _{1.6} SH _{1.78}
(b) Effect of temperature on composition of cementing phase, 3 years curing											
CaO:S _{raw} = 1:1 cured at 50 C	23.1	3.30	3.20	16.50	11.30	53.60	1.10	2.6	45.3	4.60	C _{1.8} SH _{1.8}
Similar paste as above, curing at room temp.	23.2	3.10	3.50	16.60	13.30	53.80	1.00	2.7	45.1	5.0	C _{1.4} SH _{1.8}
(c) Effect of initial consistency of the paste on the composition of the cementing phase											
CaO:S _{raw} = 1:2 wet consistency	21.77	3.8	3.9	13.57	6.16	36.0	1.3	3.1	27.0	4.6	C _{3.4} SH _{1.8}
Same composition as above, medium consistency	21.52	4.4	6.35	10.77	4.98	35.9	1.47	5.0	26.2	3.23	C _{2.3} SH _{1.8}

3 C/min to determine if there was any stepwise dehydration at any definite temperature, indicating the presence of fixed water molecules with the calcium hydrates at different temperatures. Figure 4 was derived from the dehydration thermograph.

DISCUSSION

The specific gravity of samples S-1, S-3, and S-4 in the raw state are quite low (Table 2) compared to 2.65 for quartz, indicating the existence of appreciable amounts of (a) structural or adsorbed water or (b) microscopic or totally enclosed pores, or both. In general, there is some increase in specific gravity during calcination; but the

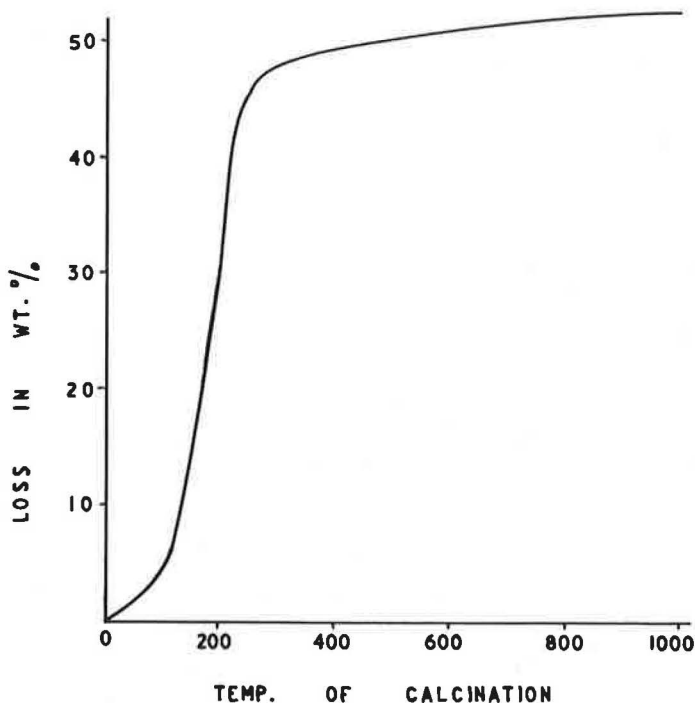


Figure 4. Dehydration curve derived from thermobalance results for S-3 (raw) lime paste.

low values even after calcining at 800 and 1000 C indicate that the second factor may contribute more than the first. The low values at 1000 C can be due to crystalline transformation to a more open structure like cristobalite in some of these cases.

The surface area (Table 3) and the calculated particle size from bound water data (Table 5) lead to interesting inferences supporting some of the interpretations from specific gravity values.

The hydroxylated surface area, as determined by the methyl red adsorption method, has the limitation that it cannot give the true surface area of the particles which could more closely be determined by such methods as the gas absorption technique. It is mainly meant to determine the "hydroxylated surface area" in silica, taking into account the generally accepted view that the hydroxyl ions are held on the surface of silica particles. It cannot give the surface area contributed by capillaries and micropores that may be inaccessible to the dye molecules because of their size or because of the blocking of the pores by adsorbed water. Estimates of the surface areas of the raw silicas from the calculated ultimate particle size, assuming a density of 2.20 for hydrated silica, are as follows.

Sample No.	Surface Area from Dehydration Data (m ² /gm)	Surface Area by Dye Adsorption (m ² /gm)
S-1	363	50.2
S-3	446	84.8
S-4	1089	—
S-5	777	75.8
S-7	1306	59.8

The lower surface area by the dye absorption method indicates appreciable capillarity, which seems maximum for S-7. The dehydration characteristics as revealed by the bound water percent given in Table 4 also show the high percentage of bound water in the raw sample and the difficulty with which most of it could be expelled even after calcination at 800 C, thus giving further evidence of the high capillarity.

Methyl red adsorption surface area values, although not giving the true surface area, could be a useful indication of the general trend during dehydration. These show a gradual reduction with an increasing degree of calcination, except in the case of S-7 which shows a gradual increase in surface area, possibly due to the progressive clearance of the water filled micro-capillaries, some of which may later allow dye adsorption.

Particle size analysis (Table 5) shows that the growth in grain size beyond 600 C is greatest in S-1 and S-4, moderate in S-3, low in S-5, and very low in S-7.

The lime reactivity results given in Table 6 show that despite a slight reduction in reactivity for samples calcined at 800 C compared to those treated at 600 C, there is a very marked increase in reactivity after calcination at 1000 C. That this should happen despite a reduction in surface area shows that certain factors having greater influence than surface area are operating in this range of calcination.

X-ray studies reveal certain correlations between the structural changes in the silicas and their reactivity with lime. The silica samples S-1, S-3, and S-4 calcined at 800 C all show a clear band in the region of 3.9 to 4.7 Å, typical of most silica gels and indicating a random structure. Thus it is reasonable to expect that up to 800 C there is essentially no structural change, and this is generally supported by existing literature, which at best indicates only certain physical changes such as size growth (also given in Table 5).

Calcination to 1000 C brings about noticeable transformation effects for the foregoing samples. In the case of S-1, in addition to the persistence of the strong band mentioned, two clear, strong lines at 3.32 and 4.19 Å showing partial crystallization to quartz structure are visible. In this case, the transformation is in progress and not

complete, and according to the principles of reactivity of solids, this state of material should be conducive to increased reactivity. This is also confirmed by the increased micro-cube strength for S-1 (1000 C) in Table 6. That this should occur despite an increase in particle size (Table 5) again proves that the structural change effects outweigh the other physical effects such as growth in size. This is in conformity with Hedval's (5) principles of reactivity of solids.

Similar effects occur in samples S-3 (1000 C) and S-4 (1000 C), the only difference being that in these cases, the transformation is towards cristobalite structure as indicated by the emergence of a clear line at 4.01 Å in the midst of the persisting band 3.9 to 4.7 Å. Here again, the crystallization is partial and incomplete, and this process of transformation results in increased reactivity (Table 6) at 1000 C despite an increase in particle size (Table 5) on the same basis as in S-1.

An interesting contrast is S-5 for which diffractometer patterns for the range $2\theta = 20$ to 25 C are available for samples heated at 600 and 1000 C. The poor pattern for S-5 (600 C) in contrast with the well crystallized cristobalite peak for S-5 (1000 C) is shown in Figure 1. In a similar way, the S-5 (1000 C) lime paste pattern (Fig. 2) is characterized by very sharp lines at 4.01 Å, 2.49 Å and weak lines at 3.11 and 2.86 Å for unreacted silica in the cristobalite form. The lines for unreacted lime occurred at 4.92 Å (medium) and 2.63 Å (strong) and some lines for a tobermorite-like mineral appear with a band of medium intensity at 10.8 to 11.4 Å region and the medium line 3.04 Å. In the case of S-5 (600 C) lime paste pattern (Fig. 2), there are no lines for unreacted silica or lime and the lines for tobermorite-like minerals are more prominent.

From the foregoing patterns, it is reasonable to infer that in the case of S-5, while the typical silica gel structure persists at 600 C, calcination to 1000 C results in complete transformation to a comparatively more stable, crystalline structure, namely that of cristobalite; and this complete transformation to a more ordered structure results in appreciable reduction in reactivity (Table 6).

To summarize, the exact effect of calcination of silica gel to 1000 C on the lime reactivity depends on the state of crystallinity of the silica after this treatment. The reactivity may be enhanced if a crystal transformation from the gel to a quartz or cristobalite structure has started or is partially completed. However, reactivity would be reduced if this transformation were completed and the better ordered crystalline silica structures were crystallized.

It has been mentioned concerning the reaction products with lime in lime-silica pastes that in the case of S-5 (600 C) and S-5 (1000 C) the lime-silica paste showed the presence of tobermorite-like minerals, these being more abundant in the case of S-5 (600 C) lime paste. The formation of such compounds is also suggested from the pattern for S-3 (1000 C) lime paste where peaks of medium intensity at 13.9, 12.3, and 11.4 Å were recorded. Some unreacted lime is also indicated by a weak line at 4.9 Å. The pattern unfortunately was not taken below 3.3 Å.

Patterns taken for S-3 (raw) lime paste of CaO:SiO₂ ratio 1:1 and 1:4 and cured at 50 C for about 4 years both showed patterns for a CSH mineral similar to riversidaite. Even in the lime rich mix, there is no evidence of a lime rich cementing phase. A careful study of the pattern reveals little free lime, suggesting that excess lime is being held in some way. Lime-silica pastes S-4 (600 C) and S-4 (1000 C) also show the strong line for a CSH compound. The weak cristobalite line visible in the 3.9 to 4.7 Å band is no longer visible in the pattern for S-4 (1000 C) lime paste, indicating that the cristobalite has been consumed in the lime-silica reaction. This evidence tends to prove that lime-silica reactions have the maximum intensity when the crystallinity of silica is poor and defective either naturally or after phase transformation reactions.

Electron micrographs for S-4 (1000 C) lime paste, S-3 raw-lime paste and S-3 (1000 C) lime paste reveal the following.

The formation of reaction products on the surface of particles of silica leading to their cementation is indicated in most of the figures through the appearance of frilled outlines on the peripheries of the particles. The interaction of the finely divided silica and lime in the vicinity of larger particles are also visible in certain areas. Some of the particles observed show resemblance to the sheet-like foils of tobermorite given by Grudemo (6).

The figures also suggest gradual breakdown of the larger silica particles, starting from the surface, to smaller particles probably resulting from the alkaline surroundings and the interaction with lime to form calcium silicate hydrates. Structural disorder in the silica, whether from structural transformation or mere hydration effects on the surface, will introduce further strain in Si-O bonds, facilitating their easy rupture under the high OH ion concentration, thus reducing the particle size and enhancing reaction with lime to form CSH compounds.

Except for the cloudy, montmorillonite-like reaction products suggesting crinkled foils of CSH compounds similar to tobermorite, the electron micrographs do not indicate the presence of the rod-shaped or broom-shaped C_2SH compounds similar to hillebrandite, and this independently suggests the formation of tobermorite-like minerals alone, which is confirmed by X-ray analysis as previously discussed.

Chemical analysis of the silica-lime reacted pastes reveals further interesting features. Table 9 gives the results of analysis of lime-silica pastes prepared from S-3 and S-4 samples calcined at 800 and 1000 C. The indicated C/S ratios in the reaction products are generally 1.1 to 2.4. The significance of some of the unconventionally high ratios is discussed later.

The effects of long-term curing of lime-silica paste at both the normal room temperature and under somewhat accelerated conditions are given in Table 9. It is reasonable to assume that the compositions of the reaction products are those of the more or less stabilized, final reaction products. Thus they appear to be around $C_{1.5}SH_{1.4}$, near that of the $CaSiH$ gel, there being no difference between curing at room temperature or up to 50 C.

The effect of initial consistency of the paste on the composition of the reaction products was studied in the case of S-4 (1000 C) lime paste (Table 9), and it was confirmed that the initial consistency had little effect on the composition of the calcium silicate hydrates formed.

The discussion so far given has revealed that during lime-silica paste reaction, calcium silicate hydrates similar to poorly crystallized tobermorite minerals are formed. These are the main cementitious compounds also formed during the hydration of portland cement under normal conditions of temperature and pressure. It has also been revealed that the rate of reaction and consequent strength development are dependent more on the state of crystallinity and the structural orderliness of the transformed or partially transformed forms of silica. The following questions still need to be answered:

1. Could the strength development in lime-silica pastes be entirely attributed to pozzolanic reaction?
2. To what extent could the composition of the cementing phases reported in Table 9 indicate the true composition of these compounds?
3. Is there a possibility of the formation of calcium silicate hydrate compounds with definite stages of hydration as in crystalline salts like $CaSO_4$ with different molecules of water of hydration?

Regarding the first question, the results of a number of experiments (Table 7) indicate that a small percentage of the strength also comes from other sources, even though the major contribution is from pozzolanic reaction. The micro-cube test results using pure S-3 paste without lime show that a small but significant strength of 320 psi was obtained, whereas in the regular micro-cube test with silica and lime the strength is about 2000 psi and more (Table 8, S-3). This strength development can be attributed to the rehydration effects on the siloxane surfaces of the silica under the conditions of the continued presence of moisture, leading to formation of silanol groups and the subsequent condensation of the surface OH groups to form a continuous network of silica gel (3). Hydrated silica particles derived from the fragmentation of the original particles by lime attack could also undergo condensation effects. Silica gels of high molecular weight so formed may lead to the cementation of silica particles composed of an unhydrated core and a hydrated surface, the core forming the framework and the hydrated silica on the surface of different particles undergoing a condensation reaction and forming a continuous cementing media. When the rehydration process proceeds so far as ultimately to convert the core to hydrated silica through continued diffusion of OH ions,

the ultimate condition will be a highly dispersed and viscous silicic acid gel of high molecular weight and little inherent strength.

The picture of cementation process involving cemented hydrated rims around unhydrated hard cores could be extended to the physical structure of sandstones and to hardened portland cement pastes, mortars and concretes. In artificial reproduction of the condition in sandstones, the results for S-3 plus quartz powder without lime show a high strength of 1,468 psi (Table 7). In all these cases, the hard quartz or aggregate particles or the unhydrated cores form the strong framework which is kept well cemented and stable by the comparatively weaker cementing phase, resulting in ultimate high strength of the mass. The applicability of the sandstone analogy could be further supported by the fact that some of the ancient Roman lime-pozzolan mortars subjected to continual leaching action by the sea currently show a composition of the cementing phase which is essentially that of pure hydrated silica (7). Under similar leaching action, the final hydrated compounds in portland cement have also been approaching the composition of hydrated silica (8).

Another important finding from the sandstone example is that even a small amount of the cementitious material forming a thin coating over the gritty particles can impart high strength to the bound mass. In many sandstones the percentage of soluble silica is surprisingly low; similarly, the analysis of the lime-silica pastes, as given in Table 8, indicates that the percentage of soluble silica, which is an index of the cementing phase, is small in most cases. This fact has also been noted by previous researchers, some of whom have wondered how this small percentage of the binding phase could impart such high strengths.

Stocker (9) worked out for a similar problem of soil stabilization the problem of how a small percentage of added binder brings about the stabilization of the soil mass. According to his calculations, a 32-Å thickness of CSH compound is sufficient for this purpose. This being so, the amount of lime actually needed for the formation of calcium silicate hydrate binder compounds is also small, and what is normally provided in lime-pozzolan mixture is far in excess of the actual requirement. Thus the strength results in Table 7 with up to 50 percent of the lime replaced by CaCO_3 still show fairly high strength values. With 100 percent calcium carbonate however, there is practically no pozzolanic reaction. The small strength of 136 psi may be merely due to the condensation effect of the silica part in the mixture containing 1 part of S-3 and 2 parts of calcium carbonate; the strength is about a third of that of the S-3 silica paste alone which is reasonably close to the value obtained. This indicates that from practical considerations, a lime with even 20 percent carbonation may still form mortars of sufficient strength with a reactive pozzolan.

Table 8 also indicates that in addition to the apparently small percentage of calcium silicate binder in pastes, there is little correlation between the amount of soluble silica and the strength developed. In most cases, before reaction with lime the silica samples by themselves contained little soluble silica. This could probably be explained by the suggested breakdown of the silica particles to smaller fragments during attack by OH ions as discussed earlier. It is the fragmentation, surface hydration, and reaction with lime-forming soluble calcium silicate hydrates that result in increased soluble silica in pastes in which the silica component originally had none. The "nibbling" of silica from the surface and the sizes of the "chunks" formed during OH attack depend on the degree of structural strain on the surfaces and the inner Si-O bonds to which the OH ions have access by the process of diffusion; the greater the strain the easier the rupture. More than the quantity of the silica so removed, it is the number of "reactive spots" and the surface OH groups these contain, the amount of actual calcium silicate hydrates formed, and the proper distribution of the cementing phase in the mass which are of greater importance for strength development. As these could vary widely, it is not surprising that there is no correlation between the dissolved silica and strength, except for a very broad trend, for any particular paste with the passage of time, indicating a general increase in strength with the formation of increased CSH compounds which is reflected by increased dissolved silica values.

There is also the possibility that formation of calcium silicate hydrate need not be preceded by the process of dissolution of silica. This could happen in a solid state

reaction involving diffusion of calcium ions through a distorted silica structure as in microcrystalline quartz or cristobalite during the initial stages of formation. In these cases too, the percentage of soluble silica in the silica samples is likely to be low and can bear little relationship to the high strengths developed.

Regarding the true composition of the cementing phase as compared to what is indicated in Table 2, it could be stated that the composition nearest to the final, stabilized composition are those from long-term reactions such as the analysis of three-year-old paste that indicates the composition $C_{1.5}SH_{1.4}$. However, the lime held by silica as determined from the sugar method need not necessarily be the structural lime in the calcium silicate hydrate phase. It could include in addition lime that is held near the particle surface by base exchange forces and by certain chemisorption forces which are stronger than mere electrostatic double-layer forces leading to base exchange but not as strong as in chemical bonds in hydrated calcium silicates. In their studies on lime stabilization of clays Hilt and Davidson (10) suggested that the lime held by the clay particle even in early ages may be due to a mechanism of "crowding" of calcium ions around the clay surface in addition to cation exchange. This crowding may be somewhat similar to the foregoing chemisorption concept for the lime silica gel paste. This lime initially held by chemisorption may later diffuse into the silica structure ultimately to form hydrated calcium silicates as suggested by Greenberg (11). This chemisorption process is a quick process and the lime held by it will be included in the composition of the cementing phases given in Table 8. Thus the calculated composition may show a higher C/S ratio than the true composition. The seemingly high C/S ratios, perhaps due to the effect, appear to be more marked in samples calcined at the lower temperature (600 C).

Another possible reason for the higher ratio has been suggested. During the treatment of hydrated paste with dilute hydrochloric acid, a part of the silicate ions originating from the dissolving calcium silicate may polymerize rapidly before filtration is completed with the resulting reduction in the soluble silica determined in the filtrate. This could give a higher C/S ratio for the computed cementing phase than the actual. On this basis, the method adopted in this study of acid treatment of the paste avoiding subsequent alkali extraction may be open to criticism.

However, it should be mentioned that the alkali treatment subsequent to acid treatment could result in excess extraction of silica, the excess being derived from the unreacted silica of the non-cementing phase of the paste getting into solution. Steopoe (4) has pointed out the error in the method usually adopted for the determination of active components in trass. Treatment with acid followed by alkali for lime-trass mixture was shown to give too high values because of the disintegration of trass, and hence he recommended a method of treatment with hydrochloric acid of density 1.12 alone, according to the method of Florentin (12). To the objection that the hydrochloric acid does not separate the hydrosilicates completely, he has pointed out the fact that the acid completely dissolves hydrated portland cement.

This discussion should reveal that the computed compositions of the cementing phase as reported in Table 9 are not absolute compositions and may deviate from the real compositions on the higher value side of the C/S ratio. The method adopted should be of value for comparisons between the different lime silica pastes, as has been done in this study.

Regarding the third question concerning the occurrence of definite hydrates of calcium silicates, the dehydration curves by thermobalance method rule out the possibility. The curve is one showing continuous loss of water with increasing temperature without any "steps," and this suggests that there are no stages in dehydration at particular hydrates levels.

SUMMARY AND CONCLUSION

The studies show that in the case of silica gels, important structural changes occur at a calcination temperature of about 1000 C, and the state of crystallinity of the samples calcined at this temperature greatly affects the lime-silica reaction. The reactivity is enhanced if a crystal transformation to cristobalite or quartz has started or is

partially complete, but it could be reduced if this transformation has reached near completion and better ordered crystalline, silica structures have been formed. It is also shown that the structural disorders known to accompany the crystal transformations affect the lime-silica reactions more intensely than does the extent of surface area.

Chemical analysis, X-ray studies, and electron micrographs also show that during the lime-silica paste reactions, calcium silicate hydrate minerals of the tobermorite type which are similar to the cement hydration products are formed. This seems to be preceded by calcium adsorption in excess of the composition of the cementing phase during the initial stages of reaction. Two courses have been suggested for the formation of the cementing phases: (a) the rehydration of the surfaces and dissolution of silica through the rupture of the strained bonds by the OH ions, later followed by the combination with lime-forming calcium silicate hydrates and (b) the holding of the Ca ions on the surface of silica by forces of chemisorption as revealed through the estimation of available calcium oxide, which is followed by the slow diffusion of Ca ions into the silica structure. There is no evidence for the existence of definite hydrates of the calcium silicate hydrates.

Through experiments employing pastes of fine silica powders mixed with water alone, it is shown that the strength development may be partially due to the rehydration and condensation reactions in silica gels, which ultimately form a continuous network of cementing silica. This could bind the inert, hard particles and impart good strength. The unhydrated cores of silica particles could also play the part of the inert hard particles. Acid solubility experiments have shown that a very small quantity of cementitious products could bind large amounts of inert materials and there need be no relationship between the quantity of cementitious materials and the strength developed. In many cases, the silica samples are shown to contain little soluble silica before reaction with lime. A possible explanation is that the breakdown of the silica particles to smaller fragments of unpredictable sizes, and the chunks formed during the attack of OH ions through the nibbling of silica from the surface, depend on the degree of the structural strain on surfaces and the inner Si-O bonds to which the OH ions have access through the process of diffusion. With respect to strength development, the number of vulnerable spots for attack by OH ions, the exact type of calcium silicate hydrates formed, and the proper distribution of the cementitious phase in the mass are of greater importance than the quantity of soluble silica. Since these may vary widely, no correlation between the soluble silica content and strength could be developed.

ACKNOWLEDGMENT

The work formed part of the fundamental research work of the Central Road Research Institute on pozzolanic reactions and is presented with the permission of the Director, Central Road Research Institute, New Delhi.

REFERENCES

1. Shapiro, I., and Kolthoff, I. M. *Jour. of Amer. Chem. Soc.*, Vol. 72, p. 776, 1950.
2. Iler, R. K. *Colloid Chemistry of Silica and Silicates*. Cornell Univ., 1955.
3. Carman, P. C. *Trans. Farad. Soc.*, Vol. 30, p. 964, 1940.
4. Steopoe, A. *Symp. on Puzzolanas*, Central Road Research Institute, New Delhi, 1964.
5. Hedval, J. A. *Proc. Symp. Chem. of Cements*, Stockholm, p. 42, 1938.
6. Grudemo. *Proc. No. 26*, Swedish Cement and Concrete Res. Inst., 1955.
7. Steopoe, A. *Building Science Abstracts*, U.K., p. 200, 1937.
8. Patrick, W. A., Frazwer, J. C. W., and Rush, H. *Jour. Phys. Chem.*, Vol. 31, p. 1511, 1927.
9. Stocker, P. T. *Jour. Australian Road Res. Bd.*, Vol. 1, p. 13, March 1963.
10. Hilt, G. H., and Davidson, D. T. *HRB Bull.* 262, p. 20, 1960.
11. Greenberg, S. A. *Jour. Phys. Chem.* Vol. 71, p. 373, 1957.
12. Florentin, D. *Chemie et Industries Spl.*, No. 446, p. 3069, 1927.

A Model for the Kinetics of the Hardening of Portland Cement

SANDOR POPOVICS, Auburn University

A formula is proposed that describes the kinetics of the hardening process of a portland cement as a function of the C_3S content and C_3A content. The formula is the mathematical expression of a simple cement model which consists only of two hardening components and satisfies several logical conditions. The properties of the model and derivation of the formula are presented. The values calculated by the new formula are compared to experimental values of compressive, tensile, and flexural strengths published earlier, and it is concluded that the equation is applicable for the kinetics of the hardening of a large group of air-entrained and non-air-entrained portland cements with reasonable accuracy. It is also found that the specific rate of strength development can be considered as a linear function, and the specific deceleration of the strength development as a quadratic function of the C_3A content of the cement.

THE technical literature contains several proposals for the relationship between the composition of portland cement and its strength and hardening, respectively. Gonnerman was probably the first who attempted to express the strength of a portland cement mortar as a function of the four main clinker minerals for various age groups. He used a linear relationship (1). Among the other proposals (2, 3, 4) perhaps the following empirical formula is the most popular:

$$s = c_1 \log t + c_2 \quad (1)$$

where

t = age of specimen;

s = strength of specimen at a given age; and

c_1 and c_2 = factors independent of the age but dependent on the type of cement, curing, testing conditions, etc.

Values calculated by Eq. 1 can be represented by a straight line in an s vs $\log t$ semilogarithmic system (5, 6, 7). This formula is the mathematical expression of the assumption that the rate of hardening is inversely proportional to the age of the specimen; that is, the product of the age and the rate of hardening at that age is assumed to be the c_1 constant. A weakness of this proposal is that it postulates an indefinite increase in strength with the increase in age which is obviously incorrect. The other proposals are not satisfactory either for one reason or another. It may also be mentioned that an excellent study was published recently on the kinetics of the hydration of calcium silicates (8), and another on the kinetics of the hydration of portland cement (9). However, neither of these discusses the strength development.

In this paper a formula is proposed that describes the kinetics of the hardening process of a portland cement as a function of the C_3S content and C_3A content. This formula is the mathematical expression of a cement model. It will be shown that the strengths

provided by an appropriate form of this cement model at various ages are close to the strengths of a given portland cement. The properties of the model are as follows:

1. It consists only of two hardening components; the first component is the C_3S , and the second is a mixture of the other cement ingredients.
2. These two components hydrate simultaneously with differing rate but without any interaction, except that the C_3A , which is a part of the second component, may affect the rate of hardening of the C_3S . Since, however, the C_3S does not affect the strength resulting directly from the C_3A in the model, the strengths of the C_3S and the second component can be superimposed.
3. The s_0 final strength of C_3S , resulting theoretically from an infinitely long curing, is the same as the final strength of the second component.
4. The decelerations of the hardening of both the C_3S and the second component at a given age are proportional to the $(s_0 - s)$ remaining strength development at that time, but the two proportionality factors are different.
5. The proportionality factors may be functions of the C_3A content.

Thus, this model, in accordance with the technical meaning of the term "model" (10), resembles a portland cement in several but not in all respects; for instance, the composition of the model is simpler. More specifically, Condition 1 is a simplification which, however, implies the empirical observation of several investigators that there is a correlation between the strength of portland cement and its C_3S content (1, 11). Condition 2 assumes that the fractional rate of hydration of the components, with the exception of C_3S , of a given cement is the same. This is again a simplification that contradicts the observation (9). It can be regarded as a modification of the hypothesis developed (and rejected) by Copeland and Bragg that the fractional rate of hydration of all components of a given cement is the same. As far as Condition 3 is concerned, experimental data by Bogue and Lerch show that the final strengths of C_3S and C_2S are practically the same (12). Condition 4 is a working hypothesis. The gradual reduction of the rate and deceleration of the hardening can be visualized as the effect of the hydrated cement that hinders the further hardening in the specimen. Finally, in accordance with experimental data (13, 14, 15, 16), Condition 5 expresses the fact that the C_3A has a more pronounced role in the hardening of portland cement than its direct contribution to the strength which would follow solely from the hardening of C_3A .

It appears feasible to construct an electrical or mechanical model that complies with the foregoing five conditions. Such a model could then be used as an analog computer for the computation of the hardening process of a portland cement.

It is not claimed that the paper contributes to the scientific side of the hydration of portland cement. Nevertheless, it appears to have certain merits. First, it deals with strength which is one of the most important technical properties; second, the applied method is a novel one which might have further useful application in the future; and third, the proposed model represents a solution which appears superior in several respects to the comparable solutions available in the technical literature.

THE NEW FORMULA AND ITS DERIVATION

The general form of the proposed formula can be obtained from the fourth condition above. The mathematical expression of this condition applied, say, to the C_3S is the following differential equation:

$$-\frac{d^2s_1}{dt^2} = a_1^2 (s_0 - s_1) \quad (2)$$

where

- t = age of specimen at testing;
- s_1 = strength of C_3S in the cement paste at a given t age;
- s_0 = strength of C_3S after infinitely long curing;
- a_1 = parameter which is independent of the strength and age but may be a function of the fineness and composition of the cement, composition of the specimen, curing and testing methods, etc. —when the age is expressed in days, the unit for the a factor is 1/day.

If the boundary conditions that $s_1 = 0$ when $t = 0$, and $s_1 = s_0$ when $t = \infty$ are applied, then the solution of Eq. 2 can be written as follows:

$$s_1 = s_0 \left(1 - e^{-a_1 t} \right) \quad (3)$$

A similar relationship can be obtained for the hardening of the second component with an a_2 parameter. Thus, it follows from the second and third conditions that the s strength of a portland cement will be expressed by the following:

$$s - s_0 \left[p \left(1 - e^{-a_1 t} \right) + (1 - p) \left(1 - e^{-a_2 t} \right) \right] \quad (4)$$

where p designates the relative amount of C_3S in the cement (percentage/100).

Three comments should be made: (a) it will be shown that the a parameters represent the specific rates of hardening for the two components of the model; (b) the form of Eq. 4 is very similar to the formula which characterizes a certain rheological model and which is frequently used for the description of basic creep of concrete (17); and (c) the hyperbolic form recommended by Goral (3) for the s vs t relationship can be obtained from Eq. 3 by expansion into a series.

EXPERIMENTAL VERIFICATION OF THE MODEL

Eq. 4 is not directly suitable for practical calculations because it contains the s_0 final strength of the portland cement which seems a function of several variables and is usually unknown. Therefore, it is expedient to transform Eq. 4 and express the $s_{rel} = S$ relative strength in a dimensionless form rather than the actual strength. If the basis of this relative strength is the 28-day strength, then

$$S = s_{rel} = 100 s/s_{28} = 100 \frac{p \left(1 - e^{-a_1 t} \right) + (1 - p) \left(1 - e^{-a_2 t} \right)}{p \left(1 - e^{-28a_1} \right) + (1 - p) \left(1 - e^{-28a_2} \right)} \quad (5)$$

$$= 100 \frac{1 - pe^{-a_1 t} - (1 - p)e^{-a_2 t}}{1 - pe^{-28a_1} - (1 - p)e^{-28a_2}} \quad (6)$$

which does not contain the value of s_0 .

One can return to actual strength values from the relative strengths with the knowledge of the strength at any age. If this strength is the 28-day strength, then Eq. 5 or 6 can be used directly; otherwise the formulas should appropriately be transformed. Such transformed formulas are applicable, at least in principle, for the estimation of the, say, 28-day strength from the strength determined at the age of 1 day or 3 days. It should be emphasized, however, that this paper investigates the kinetics of the hardening for the purpose of which relative strength values are suitable. Also, the s/s_{28} ratio is far less sensitive than the s actual strength to variations in burning and cooling conditions, as well as differences in the mineralogical composition of the raw materials used in the cement making which factors may affect the hardening process of a cement (18). Moreover, the use of relative values is not unusual in material research. For instance, the Ramberg-Osgood stress-strain diagram (18), or a study by Hansen (19) can be mentioned where the concept of a relative modulus of elasticity is utilized advantageously.

As it has been mentioned in connection with Eq. 2, the numerical values of the a parameters are influenced by numerous variables. Therefore, only the results of such tests should be used for the experimental verification of Eq. 6 where the compound composition of the portland cement is the sole variable; that is, where the fineness, gypsum content, curing and testing methods, etc., are practically identical. Several such experiments are discussed.

Gonnerman's Experiments on Mortars

A relevant investigation on mortars of 71 different portland cements was published by Gonnerman (1) as early as 1934. The range of composition of these cements was purposely expanded beyond that of normal portland cements but all the cements had an identical SO_3 content of 1.8 percent, by weight, and fineness of approximately $1,580 \text{ cm}^2/\text{g}$ (Wagner). Based on the test results, he also presented an empirical method for the calculation of mortar strength from the compound composition of portland cement.

There are three series in Gonnerman's tests that can be used for the verification of Eq. 6. In two of them the compressive strength of the various portland cements was determined with 2-in. plastic mortar cubes of 1:2.75 and 1:4.25 mixes by weight (water-cement ratios were 0.53 and 0.80 by weight, respectively). In the third series, the tensile strength of the cements was tested with 1:3 standard sand briquets. All the specimens were exposed continuously to moisture. The strength tests were performed at ages of 1, 3, 7, and 28 days, 3 months, 1 and 2 years.

An analysis of Gonnerman's test results indicated that a_1 and a_2 can be expressed as a function of the C_3A content of the portland cement. In his particular case, these a values obtained by stepwise approximation are presented below.

1. For the compressive strength of the 1:2.75 mortars:

$$a_1 = 0.0067 \text{ C}_3\text{A} + 0.10 \quad (7)$$

$$a_2 = 0.0018 \text{ C}_3\text{A} + 0.005 \quad (8)$$

where C_3A represents the percent of the potential tricalcium aluminate in the portland cement computed according to the Bogue method (21).

2. For the compressive strength of the 1:4.25 mortars:

$$a_1 = 0.005 \text{ C}_3\text{A} + 0.10 \quad (9)$$

$$a_2 = 0.001 \text{ C}_3\text{A} + 0.007 \quad (10)$$

3. For the tensile strength:

$$a_1 = 0.04 \text{ C}_3\text{A} + 0.65 \quad (11)$$

$$a_2 = 0.007 \text{ C}_3\text{A} + 0.04 \quad (12)$$

These equations show that the value of a_1 is about 7 to 10 times higher than a_2 for these mortars within the usual range of C_3A content. Accordingly, a portland cement hardens as if the C_3S develops the full value of its compressive strength by the age of about 7 days. After that any further strength increase appears to be due only to the hardening of the second component. It may also be noted that the suitable a_1 and a_2 values are much higher for the tensile strength than the corresponding values for the compressive strength. This appears to mean that the van der Waals forces which supposedly provide the main source of the tensile strength, develop their full value much more quickly in the cement paste than do the chemical bonds. If this is actually true, it would be interesting to speculate why it is so.

The form of Eqs. 7 through 12, however, is much more important than the numerical values of the coefficients because the latter are valid, strictly speaking, only for the circumstances used by Gonnerman. The form, however, reflects the effect of C_3A with respect to the kinetics of the hardening. Namely, it reveals that the specific rate of hardening is a linear function, and, consequently, the specific deceleration of hardening is a quadratic function of the C_3A content with a reasonable degree of approximation. This relation is not restricted to the C_3A . It seems also applicable to many other factors that influence the hardening of portland cement, such as the fineness of cement and the curing temperature. If a change in any of these factors increases the early strength by increasing the specific rate of hardening, then, simultaneously, the same factor increases the deceleration of the hardening to a higher degree thus the final relative strength will be less.

TABLE 1
EXPERIMENTAL AND CALCULATED RELATIVE COMPRESSIVE STRENGTHS OF 1:2.75 MORTARS^a

Cement No.	C ₃ S (%)	C ₃ A (%)	Relative Compressive Strength (%)												
			1 Day		3 Day		7 Day		28 Day	3 Months		1 Year		2 Year	
			Exp	Cal	Exp	Cal	Exp	Cal		Cal	Exp	Cal	Exp	Cal	Exp
1	43	18	16.7	13.3	43.9	33.6	63.4	58.8	100	120.2	122.7	114.2	125.1	121.7	125.1
1 Dupl	45	20	13.2	14.1	46.4	35.2	68.7	60.6	100	115.3	119.6	109.2	121.2	111.2	121.2
2B	47	16	11.5	13.3	34.3	33.9	56.0	59.5	100	108.5	122.9	125.4	126.1	115.2	126.1
2B Dupl	42	15	11.1	12.5	33.2	32.2	55.8	57.3	100	135.9	126.4	124.5	130.6	127.0	130.6
3B	43	11	10.3	11.6	28.2	30.3	45.0	55.2	100	144.1	131.9	155.0	140.4	150.2	140.4
3B Dupl	43	11	11.2	11.6	29.2	30.3	46.5	55.2	100	141.1	131.9	154.4	140.4	149.6	140.4
4	43	7	10.5	10.7	27.1	28.3	46.4	53.1	100	136.0	137.0	145.5	155.0	151.0	155.1
5B	39	2	9.4	9.3	27.2	25.4	38.2	49.4	100	168.4	142.5	194.3	193.1	208.0	198.1
5B Dupl	51	2	12.5	9.9	37.8	26.9	57.6	51.9	100	148.0	130.4	171.8	164.9	182.3	168.3
6	41	0	8.5	9.1	28.7	24.9	43.0	49.1	100	194.0	135.0	214.9	195.8	233.0	213.1
7	42	0	7.3	9.1	28.6	25.0	44.4	49.2	100	174.1	134.0	203.5	192.8	215.0	209.5
8 ^b	27	15	8.2	10.3	27.4	26.9	41.8	49.9	100	148.4	136.8	152.0	142.6	157.9	146.6
8 Dupl	42	15	9.5	12.4	30.1	31.9	54.9	56.9	100	134.1	127.0	112.2	131.3	143.6	131.3
9 ^b	53	7	10.3	11.4	30.6	30.3	48.5	56.1	100	135.1	128.3	141.1	141.9	138.1	142.0
10 ^b	56	3	9.5	10.4	34.2	28.1	51.6	53.6	100	147.4	127.0	148.2	151.9	153.0	153.4
11	51	0	9.2	9.4	37.3	25.7	57.8	50.4	100	137.2	126.6	148.5	169.6	152.4	181.8
12	41	12	10.8	11.6	29.1	30.2	48.4	55.0	100	128.2	131.9	135.3	139.4	131.3	139.4
13	38	7	6.8	10.2	22.3	27.2	44.0	51.4	100	147.1	141.9	165.0	162.4	173.0	162.6
14	37	7	8.6	10.1	28.9	27.0	51.9	51.0	100	130.1	143.0	152.2	164.0	159.5	164.2
15	48	4	6.5	10.3	27.3	27.7	47.8	52.7	100	122.9	134.0	149.0	161.2	150.0	162.1
16	42	9	12.1	11.0	31.2	29.1	50.7	53.8	100	128.3	135.4	138.8	148.1	147.1	148.2
17	39	3	7.0	9.5	29.6	25.8	51.3	49.9	100	154.7	143.4	179.0	185.9	184.2	188.4
18	43	5	9.2	10.2	31.3	27.3	49.6	52.0	100	139.4	138.7	160.4	164.8	167.3	165.4
19	44	0	6.3	9.2	27.9	25.2	46.7	49.5	100	161.9	132.2	195.0	187.0	210.8	202.6
20	42	12	7.0	11.7	25.9	30.5	48.8	55.4	100	124.7	131.2	124.2	138.5	121.0	138.5
21	40	10	7.7	11.0	30.9	29.0	54.0	56.6	100	131.7	135.7	142.6	146.8	131.9	146.8
22	41	8	7.2	10.7	27.1	28.4	49.1	52.9	100	119.4	137.6	146.8	153.4	141.3	153.4
23	38	5	7.7	9.8	25.8	26.4	47.8	50.5	100	155.3	144.1	177.5	174.2	183.0	174.8
24	41	7	8.9	10.5	30.4	27.9	45.1	52.4	100	144.1	138.9	153.2	157.9	151.2	158.0
25	44	4	7.7	10.0	28.9	27.0	47.8	51.7	100	148.4	138.0	144.7	168.6	136.0	169.6
26	42	3	7.4	9.7	26.2	26.2	43.1	50.6	100	150.5	140.0	166.0	178.8	177.4	181.1
27	41	1	6.9	9.3	28.3	25.3	47.3	49.5	100	154.8	138.3	172.1	193.4	174.0	202.6
28	44	11	11.7	11.7	31.6	30.5	52.6	55.6	100	132.1	131.1	132.1	139.5	146.0	139.5

29	40	11	7.5	11.3	25.5	29.5	47.9	54.1	100	135.0	134.2	151.5	143.4	148.0	143.4
30	39	13	7.7	11.6	28.3	30.1	53.0	54.6	100	131.8	131.9	141.8	138.4	134.3	138.4
31	49	11	13.0	12.2	33.1	31.8	53.8	57.5	100	136.0	127.5	132.5	134.8	140.4	134.9
32	36	10	9.6	10.6	26.2	27.9	42.4	52.0	100	126.2	139.2	133.3	151.4	138.1	151.4
34	41	11	9.8	11.4	26.4	29.7	44.2	54.5	100	127.4	133.4	138.5	142.4	133.9	142.4
35	41	11	10.9	11.4	30.4	29.7	44.1	54.5	100	129.0	133.4	138.0	142.4	148.2	142.4
37	16	16	8.9	8.6	19.0	23.0	34.3	44.5	100	153.9	142.5	154.9	148.5	160.0	148.5
38A ^b	61	14	11.9	14.3	40.4	36.5	67.9	63.5	100	110.2	117.4	112.4	120.5	—	120.5
39A	31	11	10.2	10.2	23.7	26.9	38.6	50.2	100	152.6	141.8	163.4	153.1	—	153.1
40 ^b	55	11	12.8	12.8	34.6	33.2	60.6	59.5	100	112.3	123.4	129.3	129.7	131.3	129.7
41	29	7	8.1	9.3	22.6	24.9	38.7	47.8	100	167.5	152.2	177.2	177.9	166.2	178.1
42	61	7	12.1	12.0	39.1	31.6	62.9	58.1	100	128.5	122.4	142.1	132.9	130.1	133.0
43	24	3	7.2	8.3	20.4	22.6	28.4	44.8	100	190.0	165.7	232.0	232.0	242.8	235.9
44	59	3	11.5	10.5	43.6	28.4	67.4	54.1	100	137.2	124.7	165.3	147.2	172.0	148.5
45	28	0	5.9	8.5	22.0	23.3	36.2	46.4	100	221.6	151.5	256.1	247.6	248.1	274.8
46	56	0	11.0	9.5	39.0	26.0	58.8	50.9	100	127.0	123.3	139.8	159.2	153.1	169.4
47	48	15	14.3	13.2	39.0	33.7	63.8	59.3	100	122.1	123.5	119.5	127.2	121.8	127.2
48	45	13	8.9	12.3	31.4	31.8	56.2	57.1	100	121.8	127.8	121.4	133.5	131.4	133.5
49	51	9	10.3	11.9	31.3	31.1	58.6	56.9	100	115.8	128.1	115.2	138.2	115.0	138.2
50 ^b	47	4	10.5	10.2	34.6	27.5	55.6	52.5	100	173.5	135.0	220.0	163.0	224.0	164.0
51	38	2	7.6	9.3	30.6	25.2	48.0	49.2	100	186.0	143.7	220.0	195.9	218.7	201.1
53 ^b	47	10	11.5	11.8	29.4	30.7	57.4	56.2	100	126.0	130.1	142.2	139.4	148.0	139.4
54	48	10	10.9	11.9	33.1	31.0	56.5	56.5	100	121.0	129.3	113.7	138.4	119.6	138.4
57	45	15	14.3	12.8	40.1	32.8	62.5	58.1	100	143.2	125.2	137.7	129.2	—	129.2
58 ^b	62	14	13.1	14.5	38.6	36.7	68.2	63.9	100	106.1	116.9	103.3	119.9	109.3	119.9
59	52	6	10.6	11.1	33.0	29.5	51.6	55.1	100	125.9	129.8	132.2	146.5	145.0	146.8
60	55	7	16.3	11.6	37.4	30.6	58.5	56.6	100	132.7	126.8	133.0	139.5	—	139.6
60A	57	6	12.4	11.4	41.2	30.3	60.2	56.3	100	135.0	125.8	137.5	140.2	—	140.4
61	56	0	10.0	9.5	37.6	26.0	58.4	50.9	100	133.0	123.3	154.8	159.2	169.1	169.4
62 ^b	74	0	11.4	9.8	48.3	26.8	74.1	52.3	100	127.0	114.4	140.0	131.4	—	136.3
100 ^b	58	17	11.3	15.0	38.0	37.6	62.0	64.4	100	95.0	116.5	86.1	118.5	—	118.5
101	56	10	13.4	12.6	34.6	32.7	61.0	59.1	100	105.4	123.7	102.1	130.9	—	130.9
102 ^b	64	17	18.1	15.7	50.0	39.2	79.8	66.6	100	105.0	113.8	95.0	115.5	—	115.5
103 ^b	66	11	12.7	13.8	39.9	35.4	69.4	62.8	100	117.9	116.8	102.0	121.2	—	121.2
104 ^b	62	20	6.7	16.5	33.6	40.6	60.0	67.6	100	103.5	112.7	88.6	113.8	—	113.8
105 ^b	60	12	8.7	13.6	31.7	34.9	49.3	61.8	100	126.0	119.5	127.2	124.0	—	124.0
106 ^b	63	17	14.3	15.6	43.7	39.0	67.5	66.2	100	101.7	114.3	—	116.0	—	116.0
108 ^b	70	5	11.8	11.7	37.2	31.2	55.0	58.0	100	122.0	117.2	—	127.9	—	128.1

^aThe Exp experimental values were obtained from Gonnerman's experiments (1); the Cal calculated values were obtained by Eq. 6 with the following factors: $\alpha_1 = 0.0067 C_3A + 0.1$ and $\alpha_2 = 0.0018 C_3A + 0.005$.

^bThese cements were double burned.

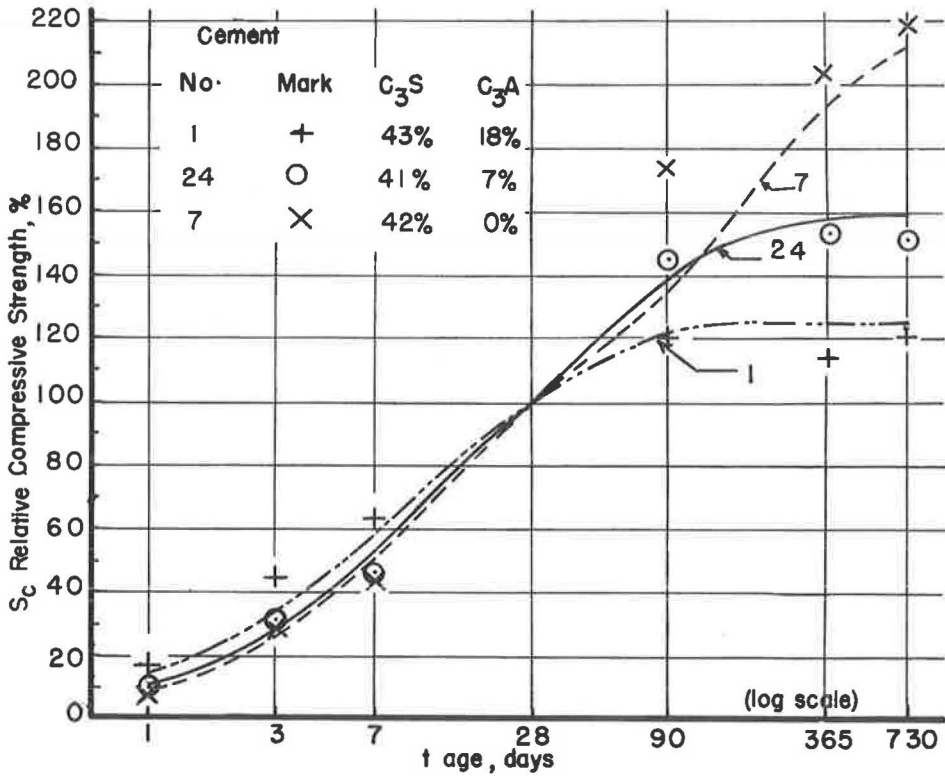


Figure 1. Comparison of experimental and computed values to illustrate effect of C_3A content on the kinetics of the hardening of portland cement in 1:2.75 mortars; experimental values represented by points, computed values by lines.

For the calculation of the factors of p , a_1 , and a_2 , the potential compound compositions of clinkers were used that were computed by Gonnerman. These factors were substituted into Eq. 6, and the values calculated by a digital computer were compared to Gonnerman's experimental values of relative strength (Table 1).

A group of the calculated values and experimental results is shown in Figure 1. The relative compressive strengths of three cements are plotted from Table 1 as a function of age. The computed C_3S contents of all three cements are practically the same but the C_3A contents are different. Points represent the experimental relative values by Gonnerman, and lines designate the calculated values. The details of the calculations are illustrated in the following.

Example 1. The a parameters of cement No. 1 are calculated by Eqs. 7 and 8:

$$a_1 = 0.22 \text{ and } a_2 = 0.037$$

Substituting these values into Eq. 6:

$$\begin{aligned}
 S_{c,1} &= 100 \frac{1 - 0.43 e^{-0.22t} - 0.57 e^{-0.037t}}{1 - 0.43 e^{-6.15} - 0.57 e^{-1.04}} \\
 &= 100 \left(1.25 - 0.54 e^{-0.22t} - 0.71 e^{-0.037t} \right)
 \end{aligned}$$

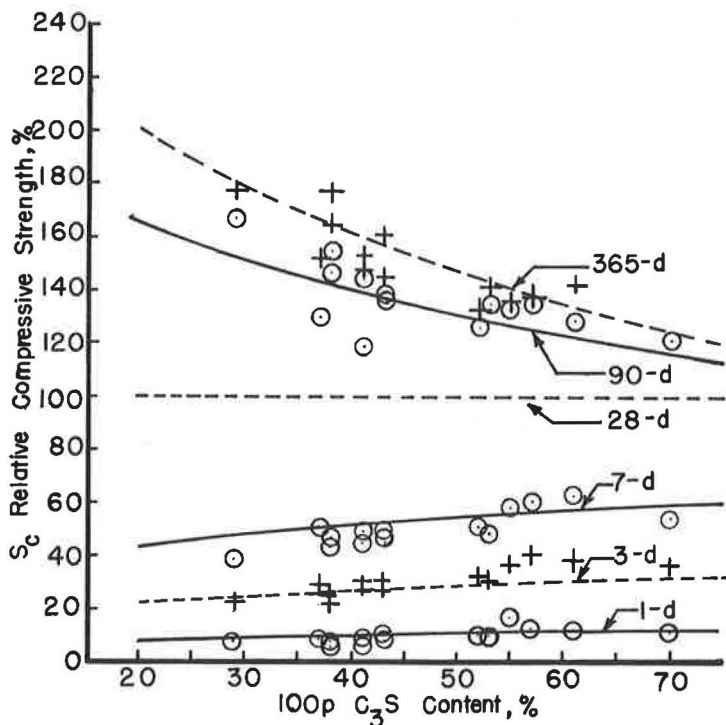


Figure 2. Experimental and computed values for relative compressive strengths of 1:2.75 mortars as a function of the C_3S content for portland cements with computed C_3A content between 5 and 8 percent; experimental values represented by points, computed values by lines.

Similarly, the equations of the curves for relative compressive strength vs age for the cements Nos. 24 and 7, respectively, are

$$S_{c, 24} = 100 \left(1.58 - 0.65e^{-0.147t} - 0.93e^{-0.018t} \right)$$

and

$$S_{c, 7} = 100 \left(2.12 - 0.89e^{-0.10t} - 1.23e^{-0.005t} \right)$$

It is apparent from these equations (or from Fig. 1) how significant the effect of C_3A content is on the strength development. Figure 1 also indicates that a straight line approximates the compressive strength vs age relationship in a semilogarithmic system within the limits of 3 and 90 days. Beyond these age limits, however, this approximation is no longer valid.

Another kind of comparison is shown in Figure 2 between experimental and computed strength values of Table 1. For this comparison, the relative compressive strength values of those portland cements are plotted as a function of C_3S content, the C_3A contents of which are within 5 and 8 percent. Again, points represent the experimental relative values by Gonnerman, and lines designate the values that were calculated by Eqs. 6, 7, and 8 with $C_3A = 6.5$ percent. Figure 2 shows that (a) there is a good correlation between the C_3S content and the relative compressive strength at various ages of cements with approximately the same C_3A contents; and (b) the model provides the relationship with a fair approximation.

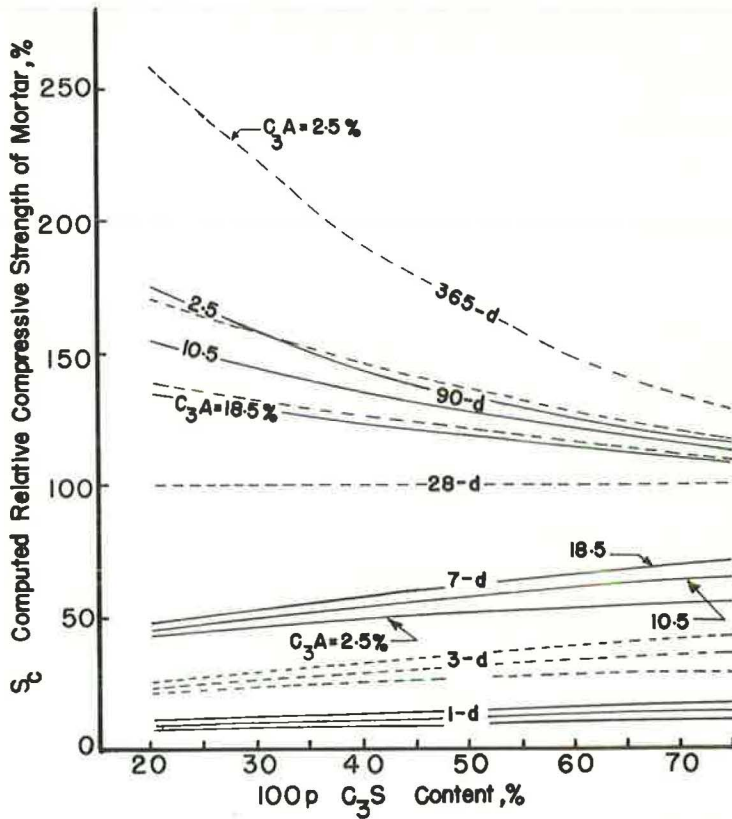


Figure 3. Effect of the C_3A content on the relative compressive strength of 1:2.75 mortars at various ages (computed values).

For other C_3A contents the relationship of strength vs C_3S content will be different, as shown by Figure 3. Relative compressive strength values calculated by Eqs. 6, 7, and 8 are presented as a function of the C_3S content for various C_3A contents and ages. In the families of curves related to the ages of 1, 3, and 7 days, the lower curves, the middle curves and the upper curves represent the C_3A contents of 2.5 percent, 10.5 percent, and 18.5 percent, respectively. This order is reversed in the families of curves related to the ages of 3 months and 1 year. Figure 3 shows that the effect of C_3A on the relative strength of portland cement depends also on the C_3S content, or that the effect of C_3S depends on the C_3A content.

The 410 pairs of strength values in Table 1 show that the agreement between the experimental values by Gonnerman and the calculated values is in most cases acceptable although high discrepancies also exist. The average difference between the experimental and calculated values, computed from the mean square residual, for these results is 11.7 percent; that is, $S_{exp} = S_{cal} \pm 11.7$. Admittedly, some of these discrepancies are due to the applied simplifications in the model. It is also true, however, that the high discrepancies occur mainly with cements that have compositions beyond that of normal portland cements, and/or where they showed retrogression in strength at later ages. For instance, if the 3-month strengths of the cements with 0 percent C_3A content are omitted as well as the 3-month, 1-year and 3-year strengths of the cements Nos. 50 and 51, then the average difference between the experimental and calculated values for the remaining 396 pairs of strength values is reduced to 9.2 percent. The goodness of fit is shown in Figure 4 by plotting these 396 pairs of strength values. The goodness of fit could further be improved by omitting those values from the comparison that show retrogression in strength.

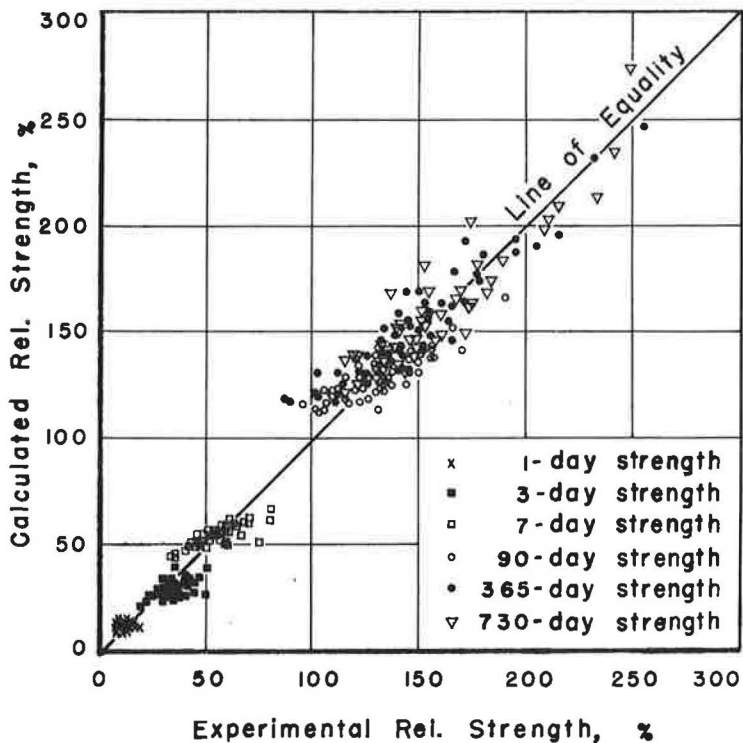


Figure 4. Comparison of 396 experimental values by Gonnerman with computed values of relative compressive strength of 1:2.75 mortars.

TABLE 2
VALUES OF a_1 AND a_2 FOR THE RELATIVE STRENGTH RESULTS BY KIEGER

Type of Test	W/C (by wt)	a_1 , 1/Day	a_2 , 1/Day
Tensile strength of mortar (ASTM C 190-49)		0.80	0.02 C ₃ A
Compressive strength of mortar (ASTM C 109-49)		0.20	0.005 C ₃ A
Flexural strength of mortar		0.45	0.01 C ₃ A
Compressive strength of concrete, 6 bag/cu yd	about 0.43	0.40	0.002 C ₃ A + 0.02
Flexural strength of concrete, 6 bag/cu yd	0.43	0.55	0.001 C ₃ A + 0.02
Compressive strength of concrete, 4½ bag/cu yd	about 0.54	0.30	0.005 C ₃ A
Flexural strength of concrete, 4½ bag/cu yd	0.54	0.5	0.005 C ₃ A
Compressive strength of concrete, 3 bag/cu yd	about 0.80	0.15	0.003 C ₃ A
Flexural strength of concrete, 3 bag/cu yd	0.80	0.25	0.004 C ₃ A

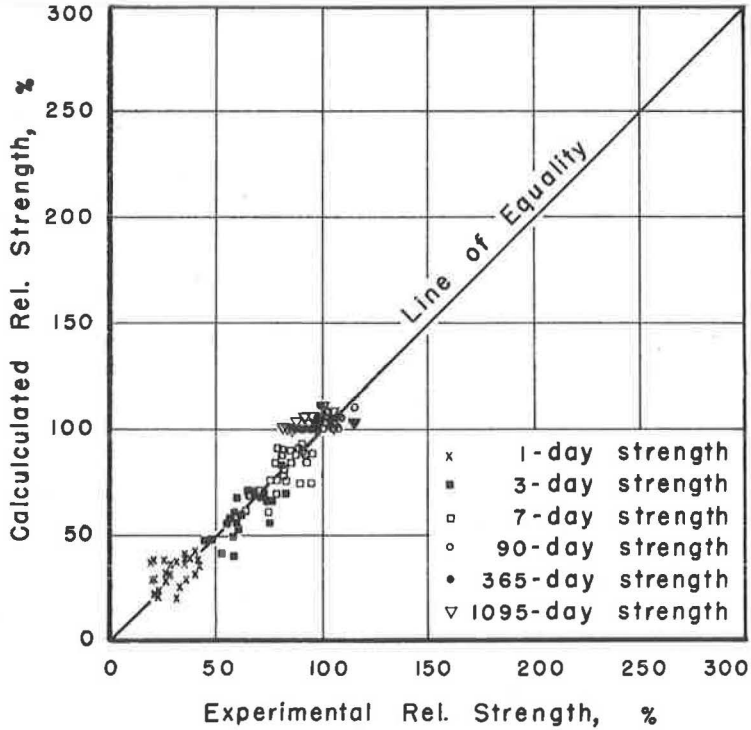


Figure 5. Comparison of 156 experimental values by Klieger with computed values of relative tensile strength of standard 1:3 mortars.

The compressive strengths of the 1:4.25 mortars and the tensile strengths show tendencies similar to the values in Table 1; however, the goodness of fit is poorer between the experimental and calculated values, particularly at the later ages. There are also cements that gave high discrepancies in the 1:2.75 mortar but showed good fit in the 1:4.25 mortar, or vice versa. This seems to indicate that some of the discrepancies are due to the random variation of the experimental results. A non-linear form for Eqs. 7 through 12 might result in a better approximation, but this would again be at the expense of simplicity.

The goodness of fit of the method recommended by Gonnerman for calculation of mortar strength in terms of age and composition of cement was also evaluated. When the calculation was extended to all 410 pairs of strength results, the values calculated by his method provided a somewhat better fit to the compressive strengths of his 1:2.75 standard mortars than the present model did. However, when the comparison was restricted to the 396 pairs of results shown in Figure 4, the goodness of fit was practically the same as that obtained by Gonnerman.

It is important to recognize that Gonnerman needed four empirical constants for each age group in his calculations. Apart from other inconsistencies, this means that his method uses more than 20 empirical constants for the detailed description of the strength development for the period of two years, as compared to the two constants (a_1 and a_2) of the model. Also, the goodness of fit of the model is improved by restricting its use to portland cements of usual composition.

Thus, one can conclude that the experimental results published by Gonnerman (1) verify Eqs. 5 through 12.

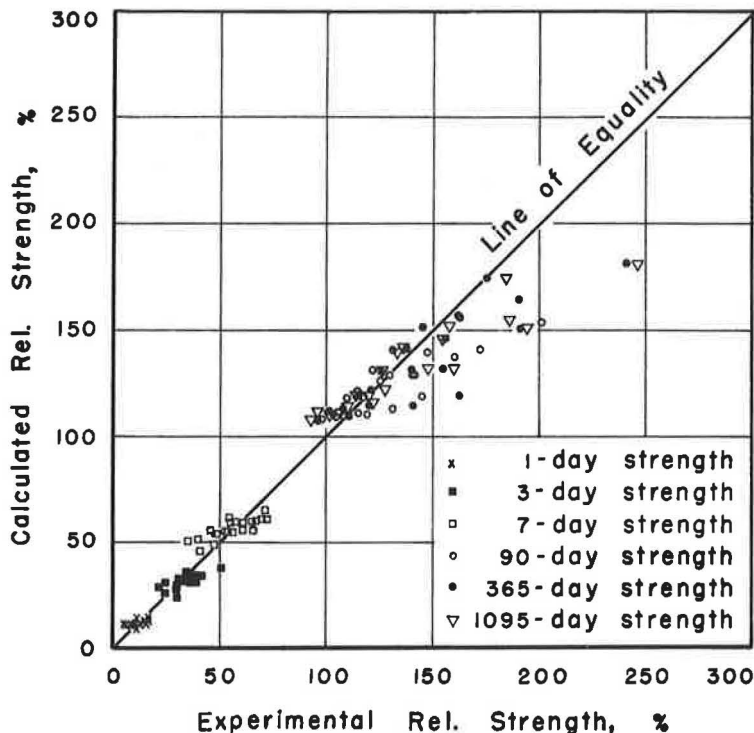


Figure 6. Comparison of 156 experimental values by Klieger with computed values of relative compressive strength of standard 1:2.75 mortars.

Experiments by Woods et al on Mortars

Woods and his co-workers have also published a relevant but short test series for mortar strength (11). The mix proportion of the mortars was 1:3 by weight, both for the compressive and for the tensile strengths. A comparison, the details of which are omitted here, indicated that Eq. 6 provides a reasonable approximation for these mortar strengths, too. More specifically, the same a_1 and a_2 values are suitable for the relative tensile strength here as were presented for the tensile strength results by Gonnerman as Eqs. 11 and 12. However, the following values were found suitable for the relative compressive strength:

$$a_1 = 0.3 \quad (13)$$

$$a_2 = 0.004C_3A + 0.01 \quad (14)$$

These values differ slightly from the values that were recommended as Eqs. 7 through 10, probably due to the difference in the mix proportions of the mortars.

Experiments by Klieger on Mortar and Concrete

Klieger tested the strength of 29 portland cements of different compositions (22). Several of these cements were "treated"; that is, these cements are comparable to the present-day air-entraining cements. The first digit of the cement numbers he used indicates the standard type of the cement. For instance, cement No. 11 is a Type I portland cement.

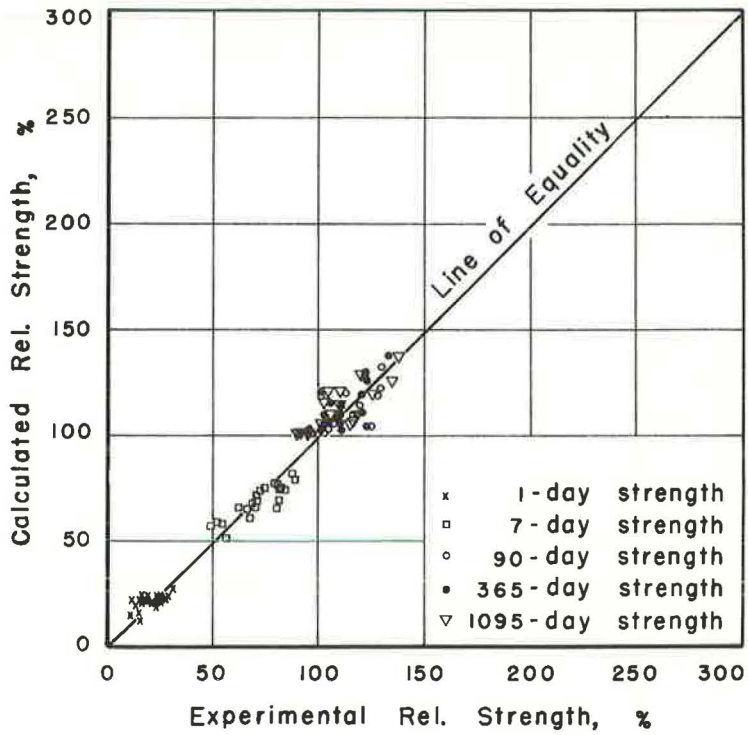


Figure 7. Comparison of 130 experimental values by Klieger with computed values of relative flexural strength of 1:2.75 Ottawa sand mortars.

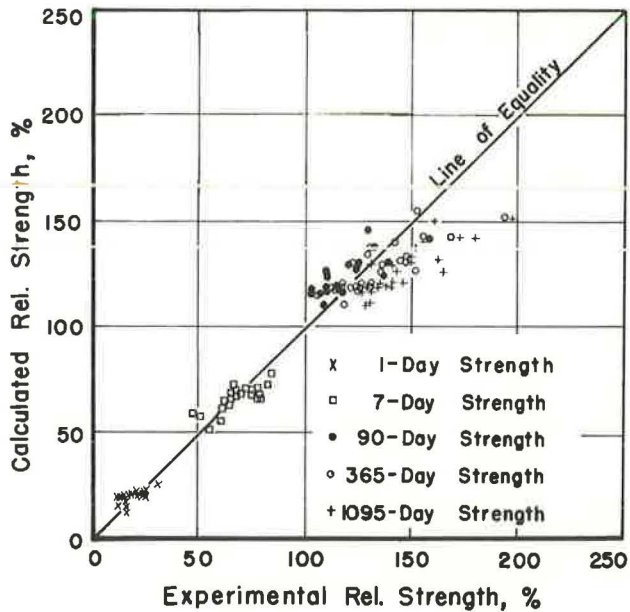


Figure 8. Comparison of the experimental and computed values of relative compressive strength of the 6 bag/cu yd concrete (experimental data by Klieger).

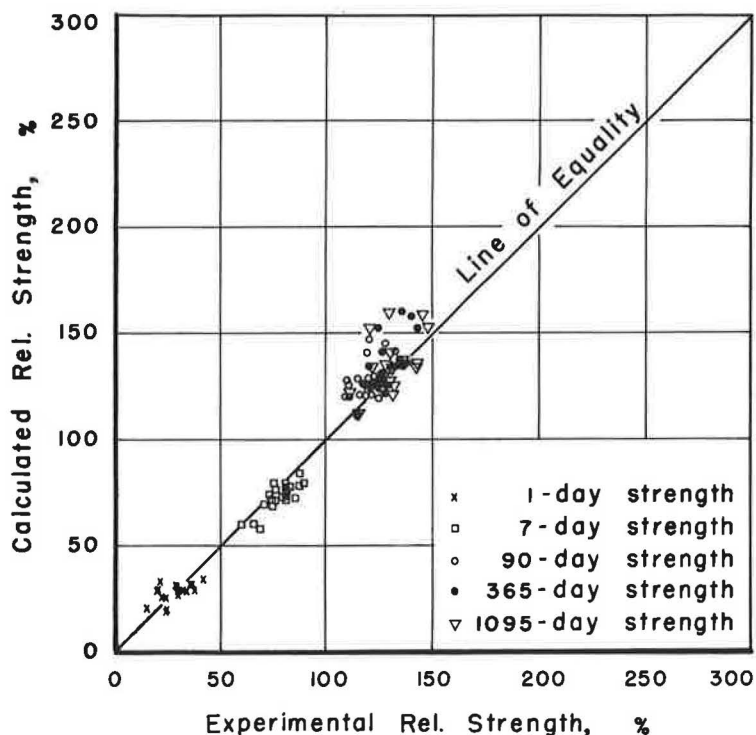


Figure 9. Comparison of 130 experimental values by Klieger with computed values of relative flexural strength of 6 bag/cu yd concretes.

In the mortar series the tensile strength was tested on 1:3 standard Ottawa sand briquets according to ASTM C 190-49; the compressive strength was tested on 1:2.75 graded Ottawa sand plastic cubes (2 in.) according to ASTM C 109-49; and the flexural strength on 1:2.75 graded Ottawa sand plastic prisms. The specimens were cured in moist air at 73 F until test. The characteristics of the tested cements were described by Lerch in a previous paper (23). Accordingly, the SO_3 content of the cements was about 1.6 percent by weight, and the fineness was about 1,800 cm^2/g (Wagner). Only cements Nos. 31, 33, and 33T were exceptions since they had higher fineness and higher SO_3 content. Thus, the hardening of these three cements should be discussed separately.

The compound composition of the cements, calculated again by the Bogue method (21), was also published in Lerch's paper except for cements Nos. 19A, 19B, and 19C, the compositions of which were presented by Klieger. The strength tests were performed at ages of 1, 3, 7, and 28 days, 3 months, 1 and 3 years.

The a values obtained for Klieger's mortar strengths are given in the upper part of Table 2. For usual C_3A contents these values are fairly close to, but not identical with the a values obtained for the Gonnerman mortar tests, probably because of differences in the curing temperature. Thus, values in Table 2 are valid again only under the circumstances that were used by Klieger (limits of C_3A content, fineness, SO_3 content, etc.). Under these circumstances, however, the a values in Table 2 appear suitable for the description of hardening of portland cements in Ottawa sand mortars provided that strengths are determined according to the pertinent standards.

Parenthetically, the value of a_1 for the standard compressive strengths of cements Nos. 31, 33, and 33T is about 0.5 1/day, and the related a_2 is about 0.17 1/day. Although these are only rather rough estimates, comparison with the pertinent values in

TABLE 3
EXPERIMENTAL AND CALCULATED RELATIVE COMPRESSIVE STRENGTHS OF 4½ BAGS PER CUBIC YARD CONCRETES^a

Cement No.	C ₃ S (%)	C ₃ A (%)	Relative Compressive Strength (%)												
			1 Day		3 Day		7 Day		28 Day	3 Month		1 Year		3 Year	
			Exp	Cal	Exp	Cal	Exp	Cal		Exp	Cal	Exp	Cal	Exp	Cal
11	50.0	12.1	13.3	17.5			71.6	67.3	100	108.8	109.9	119.5	110.1	117.9	110.1
11T	51.0	12.2	14.3	17.7			71.8	67.8	100	106.4	109.5	114.2	109.8	121.2	109.8
12	45.0	12.6	10.2	16.6			66.5	65.2	100	116.3	110.2	122.9	110.4	129.1	110.4
12T	46.0	12.5	7.0	16.8			61.0	65.7	100	109.0	110.1	120.0	110.4	125.3	110.4
13	50.0	10.1	18.8	17.6			57.9	66.9	100	121.8	113.3	135.2	113.9	142.5	113.9
14	42.5	8.2	15.4	16.3			67.2	63.2	100	110.0	120.6	126.0	122.3	135.7	112.3
15	64.5	12.1	21.6	20.1			81.1	73.7	100	107.8	106.8	110.3	107.0	109.1	107.0
16	53.5	7.5	17.5	18.6			68.7	68.9	100	112.0	117.6	121.4	119.5	131.1	119.5
16T	52.5	7.9	19.3	18.3			70.8	68.3	100	108.0	117.1	115.0	118.7	132.1	118.7
17	52.0	10.4	12.8	17.9			60.3	67.9	100	111.1	112.1	113.8	112.6	119.3	112.6
18	44.5	13.2	12.0	16.5			64.3	65.3	100	111.2	109.4	116.7	109.6	121.7	109.6
18T	44.0	13.2	9.2	16.4			72.9	65.1	100	105.8	109.4	114.8	109.7	120.3	109.7
19A	36.8	9.8	13.2	15.0			55.2	60.3	100	138.2	118.2	163.2	119.1	191.7	119.1
19B	48.6	9.9	13.1	17.3			62.0	66.2	100	120.5	114.1	127.2	114.8	140.8	114.8
19C	52.0	10.3	16.1	17.9			70.8	67.9	100	112.2	112.3	119.1	112.8	126.2	112.8
21	40.0	6.4	11.7	16.2			56.2	62.4	100	131.3	128.0	160.0	132.5	164.8	132.5
21T	38.0	6.6	9.8	15.7			57.7	61.2	100	128.6	128.4	150.8	132.7	154.3	132.7
22	41.5	6.6	10.9	16.5			54.4	63.2	100	116.5	126.3	128.5	130.3	139.2	130.3
23	51.0	3.7	16.5	19.9			63.9	71.6	100	123.0	128.2	134.7	141.2	141.0	138.3
24	41.0	5.4	15.8	16.9			65.2	63.8	100	124.6	131.2	138.0	138.3	141.0	138.3
25	34.0	4.7	15.5	15.7			49.5	60.5	100	140.8	139.8	164.6	151.9	170.5	151.9
41	20.0	4.5	13.2	12.1			45.6	50.9	100	153.3	155.9	179.7	174.2	177.0	174.3
42	27.0	3.5	14.4	15.0			46.6	58.1	100	185.3	153.6	223.0	180.7	245.3	181.9
43	25.0	6.2	8.9	12.8			46.7	53.4	100	146.0	139.2	177.0	146.0	185.8	146.0
43A	29.0	5.3	13.3	14.2			43.2	56.6	100	165.0	141.2	197.7	151.1	213.9	151.1
51	41.0	3.7	18.5	18.1			61.4	66.5	100	152.3	137.0	162.1	154.1	179.2	154.2

^aThe Exp experimental values were obtained from Klieger's experiments (22); the Cal calculated values were obtained by Eq. 6 with the following factors: $\alpha_1 = 0.30$ and $\alpha_2 = 0.005 C_3A$; T designates cements that are comparable to present-day air-entraining cements.

TABLE 4
EXPERIMENTAL AND CALCULATED RELATIVE FLEXURAL STRENGTHS OF 4½ BAGS PER CUBIC YARD CONCRETES^a

Cement No.	C ₃ S (%)	C ₃ A (%)	Relative Compressive Strength (%)												
			1 Day		3 Day		7 Day		28 Day	3 Month		1 Year		3 Year	
			Exp	Cal	Exp	Cal	Exp	Cal		Exp	Cal	Exp	Cal	Exp	Cal
11	50.0	12.1	31.6	24.9			83.2	72.4	100	113.5	109.9	110.5	110.1	116.8	110.1
11T	51.0	12.2	27.2	25.2			86.4	73.0	100	115.6	109.5	113.5	109.7	115.5	109.7
12	45.0	12.6	14.2	23.3			75.1	69.8	100	111.2	110.2	107.0	110.4	109.1	110.4
12T	46.0	12.5	12.4	23.6			76.7	70.3	100	118.7	110.1	122.5	110.4	117.9	110.4
13	50.0	10.1	27.7	25.2			70.5	72.2	100	118.3	113.2	128.5	113.8	128.5	113.8
14	42.5	8.2	23.8	23.3			77.7	68.0	100	117.3	120.6	121.2	122.3	118.1	122.3
15	64.5	12.1	33.1	29.4			89.2	80.0	100	109.2	106.8	109.2	107.0	102.2	107.0
16	53.5	7.5	25.2	27.2			81.6	74.8	100	116.0	117.5	117.5	119.4	118.2	119.4
16T	52.5	7.9	28.2	26.7			75.4	74.0	100	115.4	117.0	110.0	118.6	120.8	118.6
17	52.0	10.4	18.5	25.8			75.3	73.3	100	113.0	112.1	116.9	112.6	110.8	112.6
18	44.5	13.2	20.0	23.1			78.4	69.8	100	115.3	109.4	113.8	109.6	112.3	109.6
18T	44.0	13.2	17.1	22.9			82.9	69.5	100	121.2	109.5	123.0	109.7	123.0	109.7
19A	36.8	9.8	16.0	20.8			63.9	64.4	100	129.9	118.2	139.3	119.1	149.0	119.1
19B	48.6	9.9	18.1	24.8			71.6	71.4	100	117.2	114.1	125.0	114.8	123.2	114.8
19C	52.0	10.3	25.6	25.8			76.6	73.3	100	116.4	112.3	121.8	112.8	115.0	112.8
21	40.0	6.4	12.7	23.2			64.4	67.3	100	126.2	128.0	139.9	132.4	139.9	132.4
21T	38.0	6.6	15.7	22.5			73.0	65.8	100	121.7	128.4	140.8	132.6	139.0	132.6
22	41.5	6.6	14.8	23.7			66.4	68.1	100	118.7	126.3	118.0	130.2	127.3	130.2
23	51.0	3.7	21.2	29.6			72.3	78.3	100	124.2	128.1	130.0	141.1	124.2	141.2
24	41.0	5.4	22.2	24.5			75.2	69.1	100	118.0	131.1	125.7	138.3	127.3	138.3
25	34.0	4.7	19.3	22.7			59.6	65.3	100	134.0	139.8	144.9	151.9	139.3	151.9
41	20.0	4.5	16.5	16.8			53.0	54.1	100	129.5	155.8	152.0	174.2	145.1	174.2
42	27.0	3.5	19.0	21.5			54.0	62.6	100	165.0	153.6	176.0	180.7	172.0	180.9
43	25.0	6.2	9.8	17.7			52.8	56.7	100	125.1	139.2	125.1	146.0	126.0	146.0
43A	29.0	5.3	15.2	20.0			50.5	60.6	100	141.9	141.2	161.0	151.0	155.1	151.1
51	41.0	3.7	21.0	26.5			63.8	72.4	100	125.1	137.0	131.0	154.1	133.7	154.2

^aThe Exp experimental values were obtained from Klieger's experiments (22); the Cal calculated values were obtained by Eq. 6 with the following factors: $\alpha_1 = 0.50$ and $\alpha_2 = 0.005 C_3A$; T designates cements that are comparable to present-day air-entraining cements.

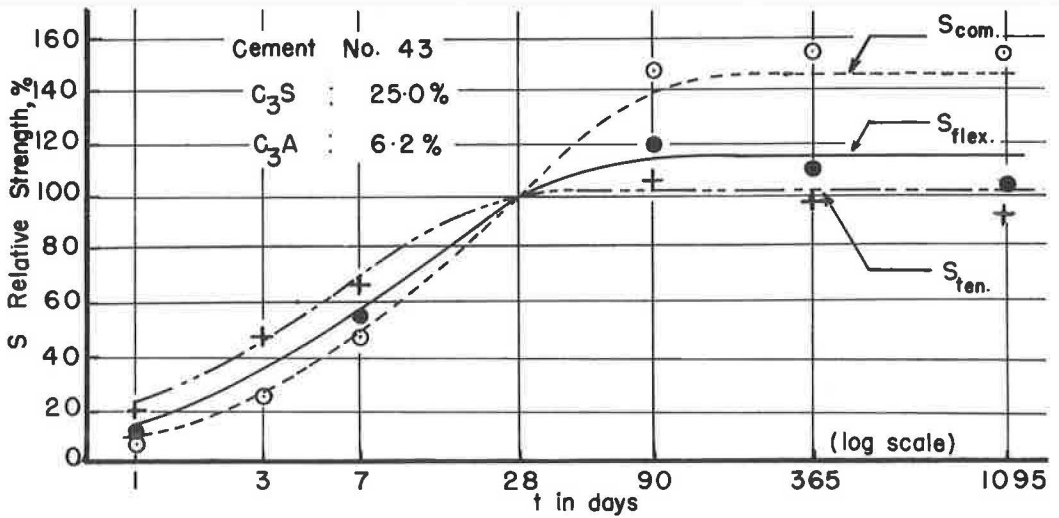


Figure 10. Comparison of experimental and computed values to illustrate effect of test method on the kinetics of the hardening of portland cement in mortars; experimental values represented by points, computed values by lines.

Table 2 shows how conveniently the a parameters can be used for the numerical characterization of the effects on the hardening of portland cements.

The a_1 and a_2 parameters were calculated for each cement with the computed C_3A content by the formulas of Table 2. These factors were substituted into Eq. 6, as in Example 1, and the calculated values were compared to Klieger's experimental values of relative strength as shown in Figures 5 through 7.

Klieger also made two large series of concrete experiments with the same cements with cement factors 6 and $4\frac{1}{2}$ bag/cu yd, respectively, and a short series with 3 bag/cu yd, all with a slump of about $2\frac{1}{2}$ in. Both the compressive strength and the flexural strength of these concretes were measured at ages of 1, 7, and 28 days, 3 months, 1 and 3 years. The flexural strength was determined by third-point loading, and the compressive strength on 6-in. beam ends with the modified cube method according to ASTM C 116-49T. All the specimens were cured continuously moist.

The a values related to these concrete strengths are given in the lower part of Table 2. The values of relative strengths that were calculated by Eq. 6 with the appropriate a_1 and a_2 values are shown in Figures 8 and 9, or for the $4\frac{1}{2}$ bag/cu yd concrete, in Tables 3 and 4, together with the relative strengths obtained from the experimental results by Klieger.

A comparison of the a values for the concretes of two different cement contents reveals that the development of relative strength is quicker and the deceleration is stronger for higher cement contents and for lower water-cement ratios, other factors being equal. Other investigations concerning the relative strength of concrete based on the 28-day strength led to the same conclusion (24, 25, 26).

The calculated values and experimental results are shown in Figure 10. The relative values of tensile strength, compressive strength, and flexural strength of mortars made with the same cement are plotted as a function of age. Points represent the experimental values, and lines designate the values calculated by Eq. 6 with the appropriate values of a_1 and a_2 of Table 2, as shown in Example 1. Again, the rate of increase in the relative tensile strength of a portland cement is much higher than the rate of increase in the relative compressive strength, but the deceleration of the development of tensile strength is also stronger.

Figure 11 shows the relationship at age 7 days between the compressive strength of mortars and the compressive strength of $4\frac{1}{2}$ bag/cu yd concretes (Table 3) made with

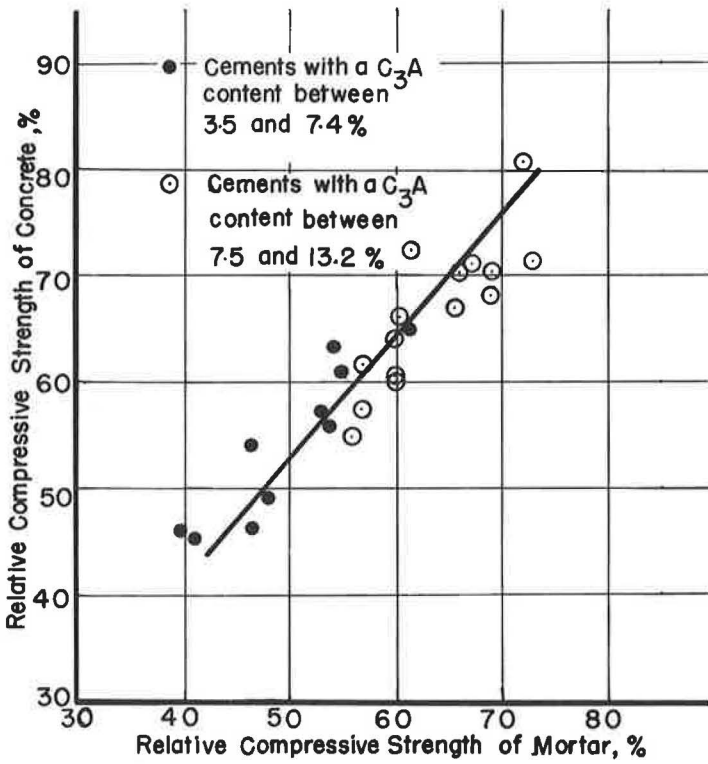


Figure 11. Relationship between the 7-day relative compressive strengths of mortars and 4½ bag/cu yd concretes made with same cements; experimental values represented by points, computed values by line.

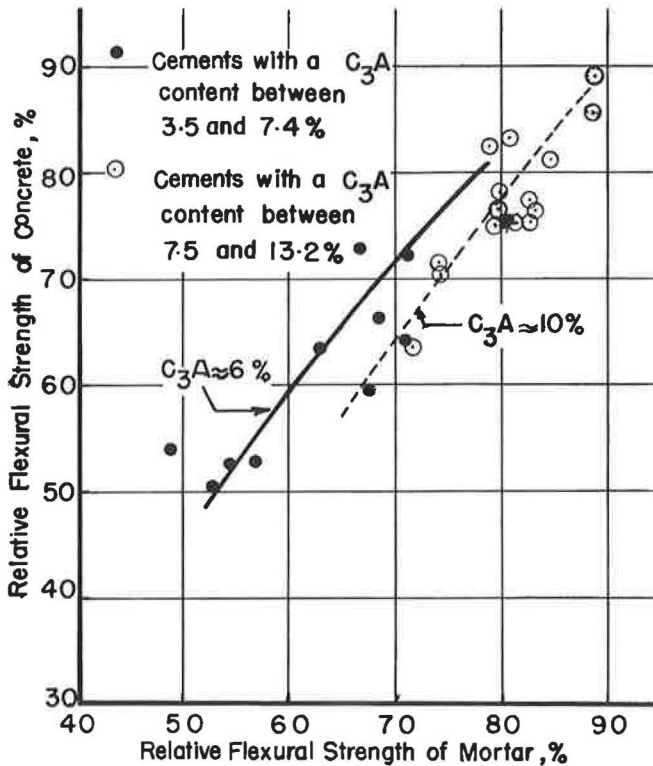


Figure 12. Relationship between the 7-day relative flexural strengths of mortars and 4½ bag/cu yd concretes made with same cements; experimental values represented by points, computed values by line.

TABLE 5
AVERAGE DIFFERENCES BETWEEN EXPERIMENTAL AND CALCULATED
VALUES FOR THE RELATIVE STRENGTH RESULTS BY KIEGER

Type of Test	No. of Exper. Values	Average Difference	Regularity of Differences
Tensile strength of mortar	156	8.2	The calculated values are apt to be slightly high at the age of 3 years.
Compressive strength of mortar	156	13.8	The calculated values for Types 4 and 5 cements are apt to be low at later ages.
Flexural strength of mortar	130	7.1	—
Compressive strength of concrete, 6 bag/cu yd	130	12.5	The calculated values are apt to be low at the age of 3 years.
Flexural strength of concrete, 6 bag/cu yd	130	9.2	The calculated values are apt to be slightly high at later ages.

the same cements. Points represent again the experimental values by Klieger, and the line designates the values that were calculated by Eq. 6 with the appropriate values of a_1 and a_2 . Figure 12 shows the relationship between the 7-day flexural strengths of mortars and $4\frac{1}{2}$ bag/cu yd concretes (Table 4) made with the same cements.

Figures 5 through 9 and Tables 3 and 4 show that there are quite a few discrepancies between the strength values calculated by Eq. 6 and the experimentally obtained values. Nevertheless, the number of serious differences is relatively low compared to the total number of experimental data given here. For the numerical illustration of the overall goodness of fit, Table 5 gives the average values of the differences between the calculated and experimental data shown in Figures 5 through 9. Further analysis reveals that the greater average differences of the compressive strengths are due mainly to the inadequacy of the calculated compressive strengths of the Type 4 and Type 5 portland cements at the ages of 1 and 3 years. Apart from these, however, the obtained overall goodness of fit does not seem inferior to the usual agreement between results of repeated strength tests. Reference is made here to the random variations in Figure 1 of Klieger's paper (22) that compares the experimental results of two tensile strength series made with the same cements.

Figures 11 and 12 provide further indirect verification of the model. They not only show that the experimentally obtained relationship between the flexural strengths of concretes and standard mortars is dependent on the C_3A content of the cement, while the relationship for compressive strength is not, but also that the model is sensitive enough to reflect these phenomena.

Thus, it may be concluded that the experimental data published by Klieger also verify the recommended model for the kinetics of hardening of air-entraining and non-air-entraining portland cements from the age of 1 day to 3 years. Exceptions are the 1-yr and 3-yr compressive strengths of Type 4 and Type 5 portland cements that the model is apt to underestimate. This also means that, within these time limits, the model can be used for the description of the hardening of standard mortar specimens with the values given in the upper part of Table 2, provided that the fineness of the cement is about 1,800 cm^2/g (Wagner), and the SO_3 content is about 1.6 percent by weight.

CLOSING REMARKS

After the completion of the first draft of the manuscript, the author learned that Eqs. 3 and 4 could also have been obtained from the assumption that the hydration of C_3S and the hydration of the second component are so-called "first order reactions." To show this, it is enough to point out that Eq. 3 is also a solution of the following differential equation:

$$\frac{ds_1}{dt} = a_1 (s_0 - s_1) \quad (15)$$

where the symbols are identical with those of Eq. 2. Eq. 15 is the mathematical definition of the term "first order reaction." This also shows that the a parameter is the ratio of the rate of hardening and the remaining strength at a given age, and as such is called the "specific reaction rate." Despite the simpler form of Eq. 15, the author kept Eq. 2, alias Condition 4, as the starting point for the development of the model. The main purpose for this was to put emphasis on the concept of deceleration of hardening which, along with the rate of hardening, contributes to a more complete picture concerning the kinetics of hardening of portland cement.

An attempt was also made to use the actual compound composition of cements rather than the potential composition for the calculation of relative strength values by the presented formulas. This was possible because the actual compound compositions of cements used in the discussed experiments of Klieger were determined by microscopic examination (27). However, the strength values calculated with these actual compositions did not show better approximation to the experimental values than when the potential compound composition was used.

Finally, results of preliminary investigations seem to support the applicability of the presented model for the description of the development of heat of hydration as well as for the relation of "maturity" versus strength of portland cement. These results will be presented in another paper.

NEED FOR FURTHER RESEARCH

The presented correlations between the calculated and experimental values are not inferior to the majority of the accepted correlations in concrete technology. On the other hand, the author does not want to give the impression by this that he is completely satisfied with the recommended model as it is, because he is not. This model is only the first step of a new attempt and, as such is necessarily crude. It is believed, however, that this method is applicable for a variety of portland cements in its present form, and seems promising enough to invite further work for the refinement of this model concept, including the development of a theory for the background of the model.

First of all, the approximation of the model for the compressive strength of Type IV and Type V portland cements at later ages is less satisfactory. It is conceivable, of course, that a modification of the model, such as a different interpretation of the factor p , or a different form of parameter a , or a change in the third condition for the model concerning the final strengths of the hardening components, or a consideration of the minor components of cement, etc., would reduce the discrepancies between the experimental results and calculated values. Thus, further research in this direction is desirable.

But besides these, numerous other questions remained open in connection with the model that can be answered only after further successful research. Several items for future research are as follows:

1. Derivation of the form of the a parameters as a function of C_3A content from theoretical considerations.
2. Determination of the effects of fineness, temperature, mix proportion, admixtures, etc., on the numerical values of the a parameters.
3. Application of the model to further aspects of the kinetics of the hydration of portland cements, such as the nonevaporable water content and specific surface of the cement gel.

4. Investigation concerning the cause of the substantial difference between the kinetics of the development of compressive strength and that of the tensile strength.
5. Application of the model for the strength of high alumina cements.

CONCLUSIONS

1. The extent of agreement between the analyzed experimental results and the values calculated by Eq. 6 is not inferior to the majority of the accepted correlations in concrete technology. Therefore, until a better method is found, it is suggested that the presented simple model is applicable for the kinetics of the hardening of a large group of air-entraining and non-air-entraining portland cements up to the age of three years.

2. The specific rate of strength development of a portland cement can be considered as a linear function and the specific deceleration of the strength development as a quadratic function of the C_3A content of the cement. The effect of the C_3S on the strength depends also on the C_3A content, and vice versa (Fig. 3).

3. The specific rate and deceleration of the strength increase are considerably greater in the case of tensile strength, than in the case of compressive strength (Fig. 10). A further analysis of this phenomenon might contribute to a better understanding of the relationship between the structure of cement paste and its strength.

4. The a_1 parameter characterizes the early strength development, while the a_2 parameter characterizes the strength development at later ages. Thus, the model appears to provide an improved tool for the numerical description of certain effects, such as temperature and admixtures, on the hardening process of portland cements.

5. The recommended model can also describe the relationship between the strengths of mortars and strengths of concretes made with the same cements with a reasonable accuracy (Figs. 11 and 12).

REFERENCES

1. Gonnerman, H. F. Study of Cement Composition in Relation to Strength, Length Changes, Resistance to Sulfate Waters and to Freezing and Thawing, of Mortars and Concrete. *ASTM Proc.*, Vol. 34, Part II, 1934, pp. 244-295.
2. Fontaine, M. Contribution a l'etude de la resistance du beton en fonction de son age (Contribution to the Study of Concrete Strength as a Function of Age). *Rilem Bull.* No. 22, Paris, March 1964, pp. 69-71.
3. Goral, M. L. Empirical Time-Strength Relations of Concrete. *ACI Jour.*, Proc., Vol. 53, Aug. 1956, pp. 215-224.
4. Hald, A. *Statistical Theory With Engineering Applications*. John Wiley & Sons, Inc., New York, 1952, pp. 541-546.
5. Hummel, A. *Das Beton-ABC (Alphabet of Concrete)*, 12th Ed. Verlag von Wilhelm Ernst & Sohn, Berlin, 1959, pp. 115-116.
6. Plowman, J. M. Maturity and the Strength of Concrete. *Mag. of Concrete Res.*, Vol. 9, No. 22, March 1956, pp. 13-22.
7. Duriez, M., and Arrambide, J. *Nouveau traite de materiaux de construction (New Treatise of the Materials of Construction)*. Vol. 1, Dunod, Paris, 1961, pp. 667-685.
8. Brunauer, S., and Kantro, D. L. The Hydration of Tricalcium Silicate and Beta-Dicalcium Silicate From 5° C to 50° C. *The Chemistry of Cements* (H. F. W. Taylor, Ed.), Vol. I, Chap. 7, Academic Press, London & New York, 1964.
9. Copeland, L. E., and Kantro, D. L. Chemistry of Hydration of Portland Cement at Ordinary Temperature. *The Chemistry of Cements* (H. F. W. Taylor, Ed.), Vol. I, Chap. 8, Academic Press, London & New York, 1964.
10. Murphy, G. *Similitude in Engineering*. The Ronald Press, New York, 1950, pp. 57, 71.
11. Woods, H., Starke, H. R., and Steinour, H. H. Effect of Cement Composition on Mortar Strength. *Eng. News-Record*, Vol. 109, No. 15, 1932, pp. 435-437.
12. Bogue, R. M. *The Chemistry of Portland Cement*, 2nd. Ed. Reinhold Publishing Co., New York, 1955, p. 672.

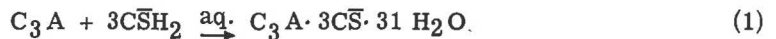
13. Bogue, R. H., and Lerch, W. The Hydration of Portland Cement Compounds. *Industrial and Engineering Chemistry*, Vol. 26, Aug. 1934, p. 837.
14. Lea, F. M., and Desch, C. H. *The Chemistry of Cement and Concrete*, 2nd Ed. Edward Arnold Ltd., London, 1956, p. 81.
15. Venaut, M. *Compte rendu d'un voyage d'etudes aux Etats-Unis et au Canada (Mai 1965) (Report of a Study Tour in the United States and Canada)*. *Revue des Materiaux de Construction, Ciments & Betons*, Oct. and Dec. 1965, Nos. 601 and 603.
16. Verbeck, G. Cement Hydration Reactions at Early Ages. *Jour. PCA R and D Lab.*, Vol. 7, No. 3, Sept. 1965, pp. 57-63.
17. Kesler, C. E., and Ali, Iqbal. Mechanisms of Creep in Concrete. *Symposium on Creep of Concrete*, ACI Publ. SP-9, Detroit, 1964, pp. 35-62.
18. Czernin, W. *Cement Chemistry and Physics for Civil Engineers*. Crosby Lockwood & Son Ltd, London, 1962, Part 3.
19. Ramberg, W., and Osgood, W. R. Description of Stress-Strain Curves by Three Parameters. *NACA*, TN 902, July 1943.
20. Hansen, T. C. Influence of Aggregate and Voids on Modulus of Elasticity of Concrete, Cement Mortar, and Cement Paste. *ACI Jour., Proc.*, Vol. 62, Feb. 1965, pp. 193-216.
21. Bogue, R. H. Calculation of Compounds in Portland Cement. *Industrial and Engineering Chemistry (Analytic Ed.)*, Vol. 1, Oct. 15, 1929, p. 192.
22. Klieger, P. Long-Time Study of Cement Performance in Concrete. Chap. 10, *Progress Report on Strength and Elastic Properties of Concrete*, *ACI Jour., Proc.*, Vol. 54, Dec. 1957, pp. 481-504.
23. Lerch, W. C., and Ford, C. L. Long-Time Study of Cement Performance in Concrete. Chap. 3, *Chemical and Physical Tests of the Cements*, *ACI Jour., Proc.*, Vol. 44, April 1948, pp. 743-795.
24. Jevtic, D. Influence de l'age sur la resistance—Quelques essais effectués avec un ciment a haute resistance initiale (Effect of Age on Strength—Experiments With a High Early Strength Cement). *Rilem Bull.* No. 5, Paris, Dec. 1959, pp. 41-48.
25. Wischers, G. Einfluss der Zusammensetzung des Betons auf seine Fruehfestigkeit (Influence of Concrete Composition on Early Concrete Strength). *Betontechnische Berichte* 1963, *Beton-Verlag GmbH, Duesseldorf*, 1964, pp. 136-151.
26. Ackroyd, L. W., and Rhodes, F. G. An Investigation of the Crushing Strengths of Concrete Made With Three Different Cements in Nigeria. *Proc. Inst. of Civ. Eng.*, Vol. 27, London, Feb. 1964, pp. 325-340.
27. Brown, L. S. Long-Time Study of Cement Performance in Concrete. Chap. 4, *Microscopical Study of Clinkers*, *ACI Jour., Proc.*, Vol. 44, May 1948, pp. 887-921.

Formation of Ettringite in Pastes Containing Calcium Aluminoferrites and Gypsum

P. K. MEHTA, Assistant Professor, and
A. KLEIN, Lecturer and Research Engineer, Department of Civil Engineering,
University of California, Berkeley

•IT IS generally believed that the C_3A phase of portland cement is the source of aluminate ions, which can react with calcium and sulfate ions to form tricalcium aluminate trisulfate hydrate ($C_3A \cdot 3\bar{C}\bar{S}$ aq.), commonly called ettringite. Portland cements contain other alumina-bearing phases, namely, the alite phase ($C_3\bar{S}$ containing generally about one percent Al_2O_3 and one-two percent MgO in solid solution) and the ferrite phase (C_2A - C_2F solid solution series to which compounds C_6A_2F , C_4AF , C_6AF_2 and C_2F belong). It was the purpose of this investigation to determine the contribution of alite and ferrite in reactions involving formation of ettringite. (Standard abbreviations are as follows: C = CaO; A = Al_2O_3 ; F = Fe_2O_3 ; S = SiO_2 ; \bar{S} = SO_3 ; H = H_2O .)

The formation of ettringite in hardened concrete is generally believed to be the most common cause of disruptive expansion. Considering the stoichiometry of Reaction 1, Hansen and Offutt (1) pointed out that the volume of ettringite formed is eight times the original volume of C_3A , whereas Bogue et al (2) showed that ettringite formed is 227 percent of the total volume of reactant solids:

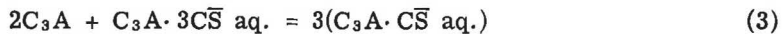
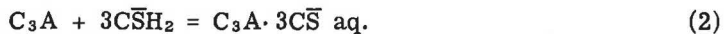


g. molar weight	270	516	1236
molar volume	88.8	222.3	714.7

Although concretes made with low C_3A cements are generally sulfate resisting, the relation between sulfate resistance and ferrite phase is not clearly established. Bogue and Lerch (3) showed that sulfate resistance of portland cements having low C_3A content but high $C_4\bar{A}F$ content could be poor.

CHEMISTRY OF SULFATE ATTACK ON PORTLAND CEMENT CONCRETES

When a sample of portland cement is hydrated with water, both C_3A and $\bar{C}\bar{S}H_2$ (gypsum) dissolve rapidly. The liquid phase becomes supersaturated with respect to ettringite through the solution of calcium, sulfate and aluminate ions, and subsequently crystals of ettringite soon appear as has recently been shown in the electron microscope investigations of Schwiete and Niel (4). The formation of ettringite in fresh concrete is not considered deleterious since the fresh material is still in a relatively unhardened state. The stoichiometry of Reaction 2 indicates that if all the C_3A is to be converted to ettringite, the gypsum content must be 1.9 times the weight of C_3A . For example, 4 percent gypsum is required to react with 2.1 percent C_3A . When the gypsum has been consumed, any additional calcium and aluminate ions which are available can combine with ettringite and form the monosulfate hydrate ($C_3A \cdot \bar{C}\bar{S}$ aq.) as shown by Reaction 3. Reaction 4, due to combined Reactions 2 and 3, indicates that the equilibrium product in concrete made with typical ASTM Type I portland cement containing about 10 percent C_3A and 4 percent gypsum, would be the monosulfate hydrate:

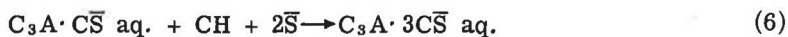


Kantro et al (5) and Chatterji and Jeffery (6) have confirmed by X-ray diffraction analyses that, in pastes of high- C_3A cements, ettringite is gradually converted to the monosulfate hydrate.

From the stoichiometry of Reaction 4, it may be calculated that 4 percent gypsum is sufficient to convert 6.3 percent C_3A into the monosulfate hydrate. In a portland cement, C_3A above 6.3 percent, reacting with water saturated with $Ca(OH)_2$, which is formed predominantly due to hydration of the calcium silicates present in portland cement, can therefore hydrate to C_4A aq. as shown by Reaction 5:



Although several investigators, including D'Ans and Eick (7), have reported the existence of solid solutions between the monosulfate hydrate and C_4A aq., Turriziani and Schipps (8) believe that the two compounds form only a series of mixed crystals. Whatever the case may be, it is evident from Reactions 6 and 7, that the presence of monosulfate hydrate or C_4A aq., or both (or a solid solution of the two compounds) in hardened concrete makes it susceptible to attack by sulfate:



Reactions 6 and 7 suggest that one method of decreasing susceptibility of cement paste to sulfate attack is through reduction in the amounts of monosulfate hydrate and C_4A aq. formed in hardened concrete. Reactions 3 and 5 indicate that this could be achieved by reducing the quantity of C_3A in portland cement. Numerous investigators including Carlson and Bates (9), Bogue et al (2) and many others have verified that there is a definite inverse relation between the C_3A content of portland cement and its sulfate resistance. The ASTM specifications (10) for sulfate resisting portland cement (Type V), therefore limit the calculated* C_3A content of the cement to a maximum of 5 percent, and calculated $C_4AF + 2C_3A$ to a maximum of 20 percent. In manufacturing cements of a fixed Al_2O_3 content, the potential C_3A content of the cement may be lowered by decreasing the A/F ratio in mix design so that more of the alumina is used up in the formation of the ferrite phase (C_4AF or C_4AF-C_2F solid solution).

As was pointed out, although concretes made with low- C_3A cements are generally sulfate resisting, the relationship between sulfate resistance and ferrite phase is not yet clearly established.

MATERIALS AND EXPERIMENTAL PROCEDURES

Table 1 gives the results of chemical analyses of three samples of commercial portland cements A, B, and C used in this investigation. These are low- C_3A or so

* The calculated C_3A content in portland cement is equal to $Al_2O_3 \times 2.650 - Fe_2O_3 \times 1.692$, where Al_2O_3 and Fe_2O_3 are determined by chemical analysis. This assumes that a part of alumina from the cement raw-mix combines with all the available iron oxide to form C_4AF phase, and the remaining alumina takes up a stoichiometric amount of lime to form C_3A . In actual practice, Von Euw (11) and Locher (12) have determined that the equivalent of about 2 percent of C_3A is present in the tricalcium silicate solid solution phase. Consequently, the potential C_3A content of cement is usually higher by about 2 percent than the actual C_3A content determined by quantitative X-ray diffraction and microscopic techniques.

TABLE 1
CHEMICAL ANALYSES OF COMMERCIAL
LOW-C₃A CEMENTS

Chemical	A	B	C	D ^a
SiO ₂	21.20	20.80	21.80	21.85
Al ₂ O ₃	2.90	2.72	2.30	4.46
Fe ₂ O ₃	5.60	5.97	6.16	5.64
CaO	65.20	65.20	65.70	62.64
MgO	1.10	1.52	0.60	0.97
SO ₃	2.40	2.43	2.63	1.96
K ₂ O + Na ₂ O	0.44	0.42	0.33	0.86
L. O. I.	1.00	0.81	0.64	1.44
Total	99.84	99.87	99.95	99.82
A/F	0.520	0.455	0.375	0.79
Potential Compounds				
C ₃ A	0	0	0	2.30
F _{SS} (C ₄ AF + C ₂ F)	15.6	15.9	15.3	17.00

^aChemical analysis of a British low-C₃A cement (19) shown here for reference only.

called zero-C₃A cements. Although the calculated C₃A content of these cements is zero, it is possible that small amounts of C₃A may be present in these cements, hence, the products of their hydration may not be truly representative of the reactions of ferrite phase alone with sulfate. It is not possible by X-ray diffraction analysis to identify small amounts of C₃A because the most intense peak due to C₃A is overlapped by (002) reflection of the ferrite phase. Consequently, in order to study the reactions of the ferrite phase with sulfate, it was necessary to make synthetic cement samples containing the ferrite phase, alite, and sulfate. Alite was incorporated into these cements so as to duplicate the conditions of hydration of the commercial cements where the environment becomes saturated with Ca(OH)₂ produced by hydration of calcium silicates.

High-purity C₆A₂F, C₄AF, C₆AF₂ and C₂F were made in a Globar furnace at about 2400 F from mixtures containing stoichiometric amounts of reagent quality CaCO₃, Al(OH)₃ and Fe₂O₃. High-purity monoclinic alite, containing stoichiometric proportions of CaO and SiO₂, and 1.0 percent Al₂O₃ along with 1.5 percent MgO was likewise made in a gas-fired furnace at 2800 F. The compounds were ground to about 3500 cm²/g (Blaine). Four samples of synthetic cements containing 50 percent alite, 35 percent of each of the above mentioned ferrite phases, and 15 percent reagent quality gypsum were prepared by blending. Another sample containing only alite and 15 percent gypsum was made in order to test whether the aluminate present in the alite contributes to formation of the calcium sulfoaluminate hydrates.

The cements were mixed with 40 percent distilled water by weight of cement, and the pastes were analyzed by X-ray diffraction at ages 3 hours, 6 hours and 24 hours. At 24 hours, the hardened pastes were stored in distilled water in a CO₂-free atmosphere. At ages 3 days, 7 days, 28 days and four months representative samples of the hardened paste were withdrawn for X-ray diffraction analysis.

The synthetic cements investigated did not include consideration of the influence of the alkalis which normally exist in portland cement, both as alkali sulfates and in case of sodium, as components of C₃A phase. According to Lea (13) concentrations of alkalis up to about one percent could occur in the liquid phase of a cement paste during the first few hours of hydration. Since the solubility of calcium hydroxide is much reduced by the presence of alkali hydroxides, Lea speculates that they might have some influence on the nature of the cement hydration products. To ascertain the influence of alkalis

on the nature of the hydrates produced by hydration of synthetic cements, another set of the four synthetic cements containing alite, ferrite phase and gypsum were mixed with one percent NaOH solution. As before, the pastes were subjected to X-ray diffraction analysis at regular intervals.

A Philips Norelco X-ray generator with a Cu-target at 40 KV and 35 mA was used in conjunction with a Philips Norelco Diffractometer having 1° divergence and scatter slits, 0.006 in. receiving slits, and a scintillation counter at 850 V. The pulverized sample was packed in an aluminum holder and was scanned at one-half degrees 20/min. The level of pulse height analysis was maintained at 8.0 V, the width at 27.0 V, and the rate meter time constant at 2 seconds. The diffraction patterns were recorded at 500 counts per second full-scale deflection by a Bristol recorder. The patterns were analyzed for unhydrated ferrite phase and trisulfate hydrate. A semi quantitative estimate of these compounds in the pastes was made by direct comparison of relative peak heights of certain intense peaks which were not overlapped by peaks of any other compound.

RESULTS AND DISCUSSION

Figures 1 through 4 plot relative amounts of the trisulfate hydrate formed (as represented by the size of the most intense peak on X-ray diffraction pattern) against age for the hydrated samples containing alite, gypsum and one of the four compositions of the ferrite phase. The lower curve in each figure shows the effect of presence of alkali in liquid phase. The peak heights are plotted to a linear scale, and age to a log scale.

Figure 5 shows similar plots for the three commercial brands of zero- C_3A cements used in this investigation.

The data in Figure 1 indicate that the pastes of synthetic cement containing C_6A_2F show trisulfate hydrate formation within three hours of addition of water, and that most of the total trisulfate hydrate present was formed within 6 hours of hydration. The peak intensity remained constant between ages 6 hours and 7 days, but in the case of

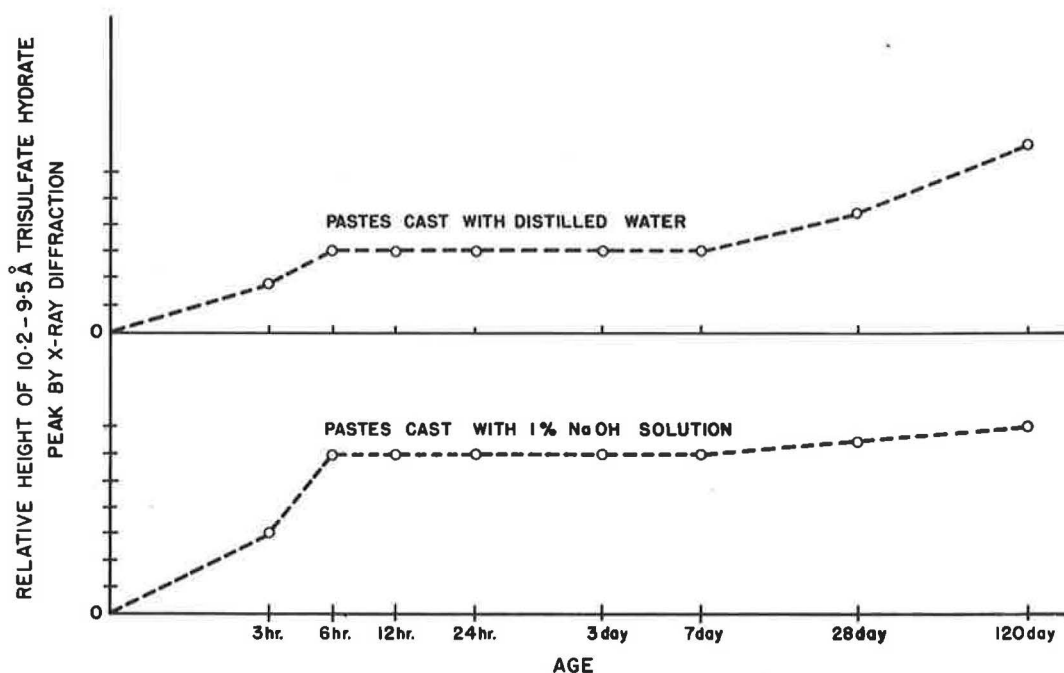


Figure 1. Trisulfate hydrate formation in cements containing C_6A_2F , alite and gypsum ($w/c = 0.4$).

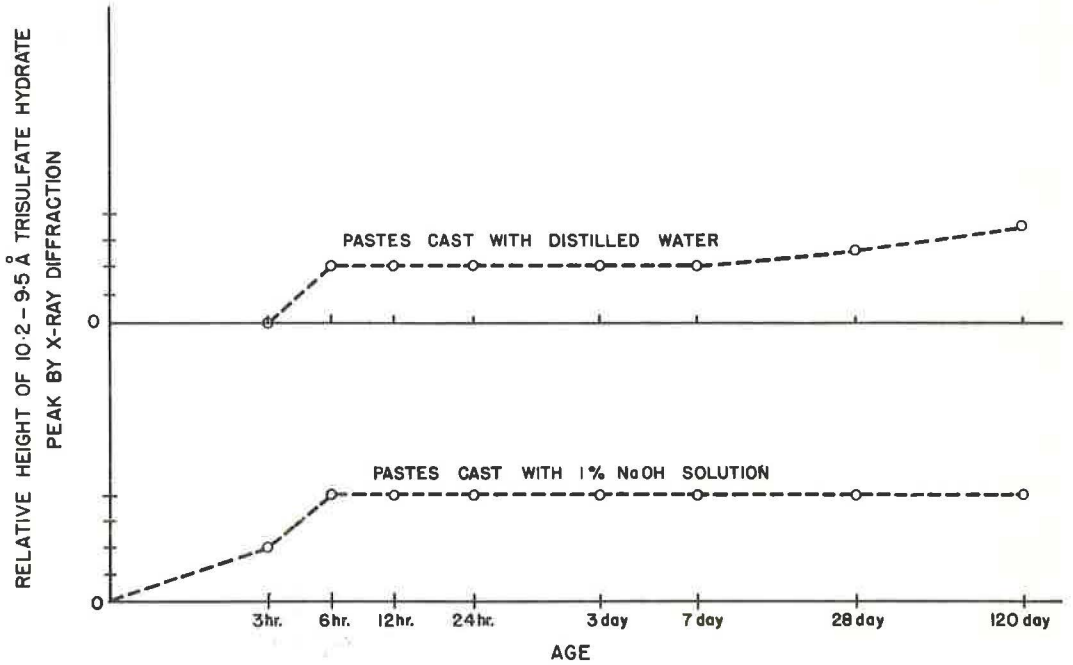


Figure 2. Trisulfate hydrate formation in cements containing C_4AF , alite and gypsum ($w/c = 0.4$).

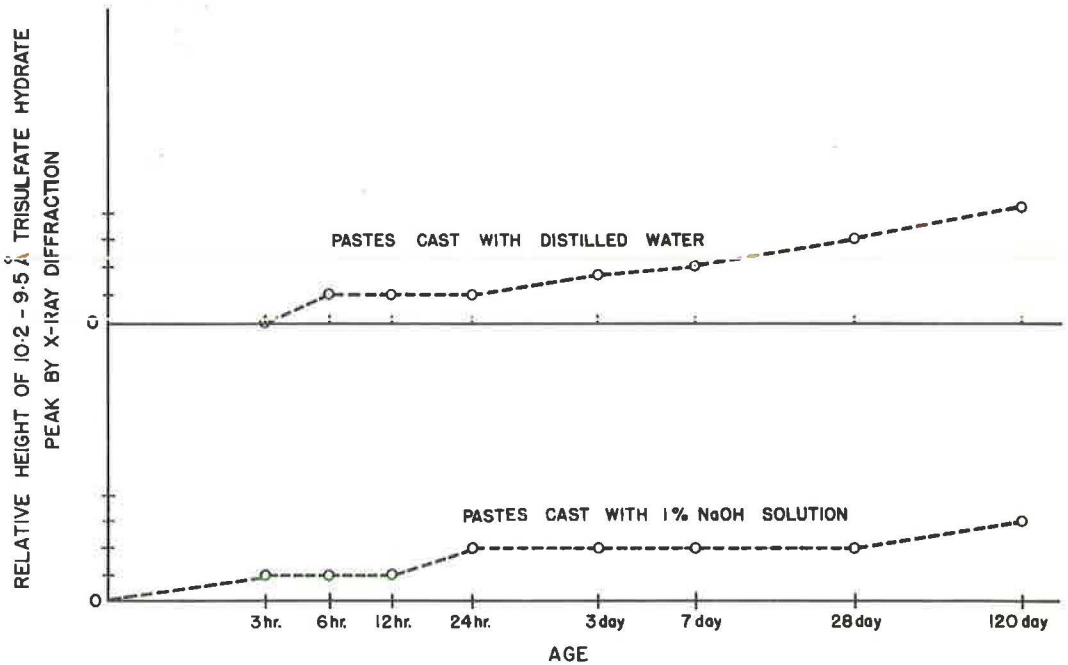


Figure 3. Trisulfate hydrate formation in cements containing C_6AF_2 , alite and gypsum ($w/c = 0.4$).

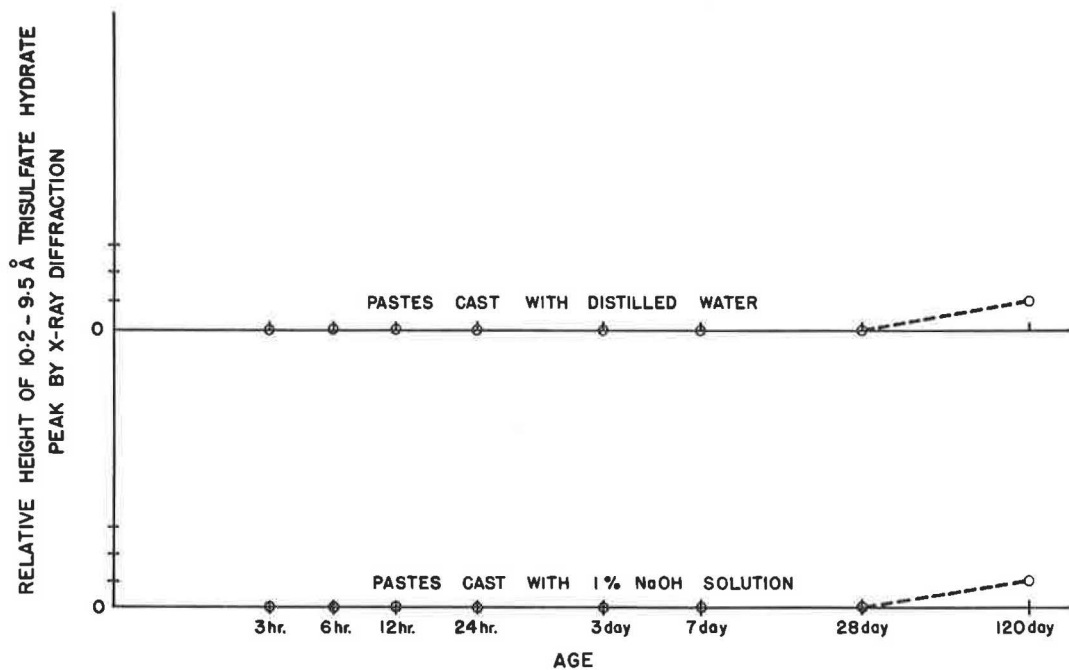


Figure 4. Trisulfate hydrate formation in cements containing C_2F , alite and gypsum ($w/c = 0.4$).

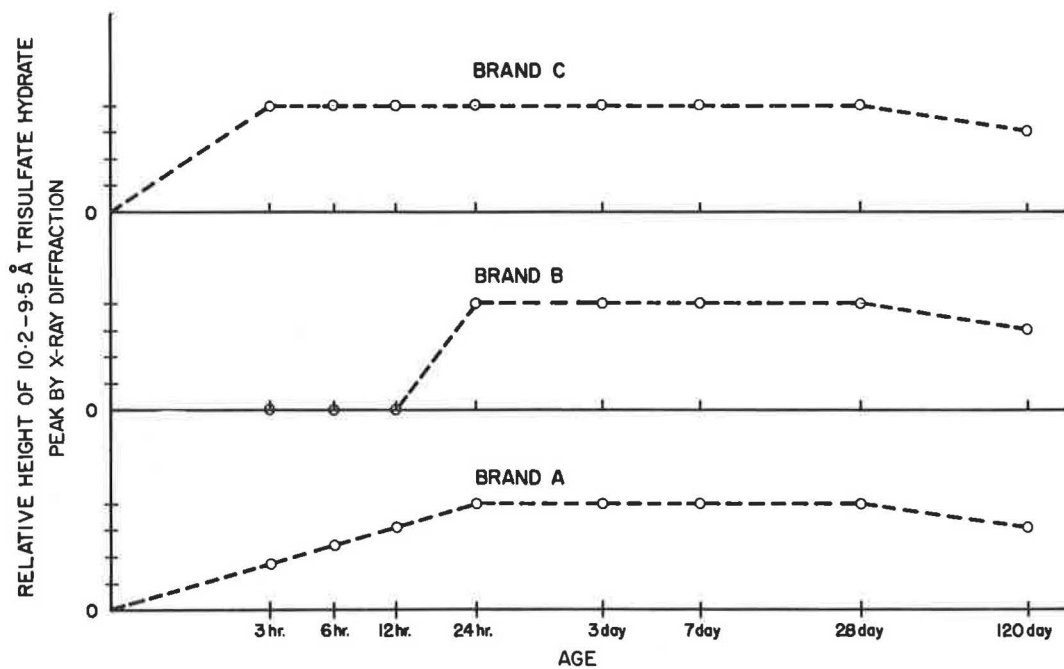


Figure 5. Trisulfate hydrate formation in commercial zero- C_3A cements ($w/c = 0.4$), pastes made with distilled water.

the samples made with distilled water, an appreciable increase in the intensity of trisulfate hydrate peak was observed between ages 28 days and 120 days. On the contrary, in the case of samples made with one percent NaOH solution, practically all the trisulfate finally present had formed within 6 hours of hydration, and no significant increase in the intensity of the peak was observed up to age 120 days. The relative sizes of trisulfate hydrate peaks at 120 days, however, were found to be similar regardless of whether distilled water or NaOH solution was used.

The data in Figures 2 and 3 for cements containing, respectively, C_4AF and C_6AF_2 are similar in qualitative nature to the data reported for cements containing C_3A_2F (Fig. 1). Quantitatively, the amount of trisulfate hydrate formed appeared to increase with increasing A/F ratio of the anhydrous phase. This shows that reactivity of the ferrite phase decreased with increasing F/A ratio. Similar observations have been reported by Carlson (14) for action of water on the ferrite phase.

Figure 4 indicates that the formation of ferritic-trisulfate hydrate on hydration of cements composed of C_2F , gypsum and alite, is a very slow process, confirming that C_2F is the least reactive of all the ferrite phase compositions. Greene (15) quotes Watanabe and Iwai as having concluded that no $C_3F \cdot 3\overline{CS}$ aq. was formed in the hydration products of C_2F and calcium sulfate. It is likely that these investigators studied the early-age hydration products only. On the contrary, Bogue and Lerch (16), and Budnikov and Gorshkov (according to Greene) did identify $C_3F \cdot 3\overline{CS}$ aq. in reaction products of C_2F with sulfate.

Figures 1 through 4 also indicate that replacement of distilled water by one percent NaOH solution for hydrating the cements accelerates the reactions but does not cause any discernible change either in the nature or in the amount of the hydration product. This is in conformity with the results of several investigators including Seligmann and Greening (17).

Figure 5 shows the data on trisulfate hydrate formation in the pastes of commercial zero- C_3A cements. The rates of formation of the trisulfate hydrate within 24 hours were observed to be different for each case, but whatever trisulfate was present in the 24-hour sample remained constant until age 28 days and, thereafter, diminished slightly as indicated by decreased height of peak at age 120 days. The decrease in amount of trisulfate hydrate was not accompanied by formation of monosulfate hydrate or any other detectable sulfate-bearing phase.

No trisulfate hydrate was detected in the hydrated alite-gypsum composition, thereby indicating that the Al_2O_3 present as a solid solution in alite is probably not extractable and, therefore, was not available for reactions with sulfates. Between 2.56 and 3.18 Å the diffraction pattern showed an increase in background which was probably indicative of the presence of poorly crystallized calcium silicate hydrates.

The (100) reflection due to the aluminate-based trisulfate hydrate occurs at 9.71 Å, whereas in this investigation, a broad peak at 10.2 to 9.5 Å was observed, especially in samples of the early-age hydrates. This could be due either to poorly crystallized aluminate-based trisulfate hydrate or to a solid solution between $C_3A \cdot 3\overline{CS}$ aq. and $C_3F \cdot 3\overline{CS}$ aq., as reported by Turriziani (18).

Regarding the sulfoferrites, it is generally agreed that both the ferritic-trisulfate hydrate ($C_3F \cdot 3\overline{CS}$ aq.) and the ferritic-monosulfate hydrate ($C_3F \cdot \overline{CS}$ aq.) which are structurally analogous to $C_3A \cdot 3\overline{CS}$ aq. and $C_3A \cdot \overline{CS}$ aq., respectively, exist under normal conditions. By X-ray diffraction it is possible to differentiate between the ferrite-based trisulfate hydrate and the aluminate-based trisulfate hydrate, because the (114), (216), and (226) reflections are apart by about 0.2 deg 2θ (cu. ka). Turriziani (18) credits Cirilli with the finding that $C_3F \cdot 3\overline{CS}$ aq. forms solid solutions with $C_3A \cdot 3\overline{CS}$ aq. up to a limiting F/A molar ratio of 3.0. Further, on the basis of Malquori and Cirilli's work, Turriziani states that, contrary to $C_3A \cdot \overline{CS}$ aq. - C_4A aq. solid solutions, no such solid solutions are formed between $C_3F \cdot \overline{CS}$ aq. and C_4F aq. Another important observation by Malquori and Cirilli is that, unlike $C_3A \cdot \overline{CS}$ aq., $C_3F \cdot \overline{CS}$ aq. does not change to trisulfate hydrate on contact with solutions saturated with lime and gypsum.

The diffraction peaks improved in sharpness with age, hence the presence of poorly crystallized trisulfate hydrate at early age cannot be ruled out. Since a small increase

in the unit cell dimensions occurs when Fe replaces Al [the (100) reflection for a synthetic preparation of $C_3F \cdot 3\bar{C}\bar{S}$ aq. being at 9.9 \AA] therefore, substitution of Fe for a part of Al might be responsible for the broadness of the peak. In his observations on the formation of cubic phase, $C_3(A, F)H_6$, by action of water on different compositions of ferrite phase, Carlson (14) stated that the unit-cell dimensions of the cubic phase obtained were larger than the dimensions of pure C_3AH . He concluded that substitution of Fe_2O_3 in the hydrate corresponded to about one-tenth of the total R_2O_3 on molar basis ($R_2O_3 = Al_2O_3 + Fe_2O_3$). Also, under conditions of paste hydration of C_4AF , the hydrate formed contained Fe_2O_3 , although Carlson reported that the hydrate was poorer in Fe_2O_3 than the anhydrous material. Consideration of the stoichiometry of the reaction shows that there is insufficient lime to combine with all the Al_2O_3 and Fe_2O_3 to form $C_3AH_6 - C_3FH_6$ solid solution phase from hydration of C_4AF . The presence of excess lime should aid this process, as was confirmed by Chatterji and Jeffery (19) who obtained the cubic phase with unit-cell dimensions about 0.5 percent larger than that of C_3AH_6 by hydrating paste of C_4AF with added lime.

Analogous to the finding of Carlson (14) on the formation of iron-substituted $C_3(A, F)H_6$ phase as previously discussed, if it is assumed that reactions of sulfates with ferrite phase in the presence of $Ca(OH)_2$ are capable of forming $C_3(A, F) \cdot 3\bar{C}\bar{S}$ aq., the stoichiometric gypsum requirements by weight for complete conversion of alumina and for conversion of one-tenth of the Fe_2O_3 present to trisulfate hydrate are, respectively, 1.55 parts, 1.17 parts and 0.82 parts per part of the ferrite phase for C_6A_2F , C_4AF and C_6AF_2 . Considering that the synthetic cements contained 15 percent gypsum and 35 percent ferrite phase by weight (i. e., 0.43 parts of gypsum per part of ferrite phase), it is evident that the amount of gypsum used is far below the requirement for complete conversion to the trisulfate hydrate, and, therefore, the availability of excess aluminate (plus one-tenth of ferrite ions on molar basis) ions should have transformed the trisulfate hydrate to the monosulfate hydrate, as shown by Reaction 3. The data from the present investigations show that this did not happen. On the contrary, the trisulfate hydrate content continued to be constant between the ages 7 days and 120 days, which indicates that reactivity of ferrite phase was greatly influenced by presence or absence of excess of $Ca(OH)_2$ in the environment.

Due to insignificant hydration of alite within the first few hours of hydration, no $Ca(OH)_2$ was detected in hydrated samples at age 3 hours. In the 6-hr samples, the first traces of $Ca(OH)_2$ were detected in every case. Accordingly, trisulfate hydrate appeared to have continued to form until the medium became adequately supersaturated with $Ca(OH)_2$. Once there was excess of $Ca(OH)_2$ in the environment, the reactivity of ferrite phase was greatly depressed so that no more trisulfate hydrate formed due to unavailability of aluminate and ferrite ions in the liquid phase. On the basis of X-ray diffraction analysis, the content of free $Ca(OH)_2^*$ in the hydrated pastes was noticed to fall appreciably in 28-120 days period during which the trisulfate hydrate content showed significant increase.

The sulfate-resistant cement used by Chatterji and Jeffery (19) (cement D, Table 1) had 2.3 percent potential C_3A and 17.0 percent potential C_4AF . Even this cement, having a relatively reactive form of ferrite phase, did not show conversion of trisulfate hydrate to monosulfate hydrate within the period of testing reported (3 months). The authors attributed this to either (a) stabilization of trisulfate hydrate crystals by the presence of free $Ca(OH)_2$, or (b) depression in the reactivity of ferrite phase to such an extent that no monosulfate hydrate was formed. Carlson (14) studied the effect of $Ca(OH)_2$ concentration on dissolution of various compositions of the ferrite phase and reported that the dissolution reaction was inhibited by increasing concentration of $Ca(OH)_2$. The data in the present investigation indicate that probably part of the reason for sulfate resistance of very low C_3A cements lies in the relatively high proportion of

* The free $Ca(OH)_2$ content of hydrated portland cements is known to decrease with age because the calcium silicate hydrate gel gradually absorbs $Ca(OH)_2$ to form products higher in CaO/SiO_2 ratio.

less reactive ferrites and also in the depressed reactivity of the ferrite phase in presence of excess $\text{Ca}(\text{OH})_2$. Although the trisulfate hydrate is less soluble in solutions saturated with $\text{Ca}(\text{OH})_2$ than in pure water, the concentration of sulfate and aluminate ions in the liquid phase also affect its stability. In the present study, the stability of trisulfate hydrate was enhanced by the presence of sulfate* ions, and by the extremely slow rate of availability of aluminate (plus ferrite) ions, i. e., slow rate of hydration of the anhydrous phases containing Al_2O_3 and Fe_2O_3 . Furthermore, just as the iron analogue of monosulfate hydrate, on contact with sulfate solutions, resists change to trisulfate form, it is possible that the trisulfate hydrate in which part of Al_2O_3 is replaced by Fe_2O_3 may resist change to monosulfate on contact with aluminate solutions.

The X-ray diffraction studies of the hydration products of commercial brands of zero- C_3A cements confirm the preceding findings for hydrated synthetic cements containing ferrite phase, gypsum, and alite. The trisulfate hydrate, formed within the first 24 hours of hydration, remains fairly stable. The small amount of sulfate present is probably responsible for the observation that not even a small increase in the trisulfate hydrate content occurred in later-age samples. As compared to the synthetic cements, the hydrated commercial cements (Fig. 5) exhibited a small decrease in trisulfate hydrate during the period of 28-120 days. Since no monosulfate formed at the cost of trisulfate hydrate, on the basis of Kalousek's (20) observations it is speculated that the SO_3 made available due to dissolution of trisulfate hydrate might have been absorbed by the calcium silicate hydrates. No hydrogarnets [$3\text{CaO}(\text{Al}, \text{Fe})_2\text{O}_3 \cdot 3(\text{H}_2\text{O}) \cdot 2\text{SiO}_2$] were detected among the hydration products of commercial zero- C_3A cements up to an age of 120 days. It is possible that at later ages hydrogarnets containing SiO_2 could be present in the hydration products of zero- C_3A cements, but investigations of Schwiete and Iwai (21) have indicated the sulfate resistance of such phases.

CONCLUSIONS

Alite and ferrite phase are the two alumina-bearing phases in zero- C_3A cements. No trisulfate hydrate was formed in hydrated alite-gypsum mixtures, thereby indicating that under the test conditions used, the Al_2O_3 present in alite is not liberated for participation in the reactions involving sulfates and aluminates. On the other hand, the trisulfate hydrate was formed on hydration of cements containing alite, gypsum, and any one of four compositions of the ferrite phase, i. e., $\text{C}_6\text{A}_2\text{F}$, C_4AF , C_6AF_2 and C_2F . The diffuse nature of the peaks was apparently due both to the poor crystallinity of the product and to participation by a portion of the Fe_2O_3 present in the formation of $\text{C}_3(\text{A}, \text{F}) \cdot 3\overline{\text{CS}}$ aq. The amount of the trisulfate hydrate formed by reaction of the ferrite phase with sulfate under the conditions of the test was observed to be greatly influenced by A/F ratio, the $\text{C}_6\text{A}_2\text{F}$ being the most reactive and the C_2F being the least reactive. Alkalies were found to accelerate the reactions, but altered neither the nature nor the amounts of the hydration products. Unlike typical ASTM Type I portland cements, the trisulfate hydrate formed from hydration of either the synthetic zero- C_3A cements or of the three commercial brands of zero- C_3A cements, did not convert to monosulfate hydrate up to age 4 months—a phenomenon which may explain the sulfate resistance of such cements. Depressed reactivity of the ferrite phase in presence of excess of $\text{Ca}(\text{OH})_2$ is, perhaps, the main reason for absence of monosulfate hydrate in the 4-month-old hydrated specimens of cements used in this investigation.

ACKNOWLEDGMENT

The research was sponsored by National Science Foundation, Grant No. 616.

* Unreacted gypsum and a large portion of unhydrated ferrite phase were present even at age 120 days.

REFERENCES

1. Hanson, W. C., and Offutt, J. S. Gypsum and Anhydrite in Portland Cement. U. S. Gypsum, p. 26, 1962.
2. Bogue, R. H., Lerch, W., and Taylor, W. C. Industrial Eng. Chem. Vol. 26, p. 1049. 1934.
3. Bogue, R. H., and Lerch, W. Portland Cement Association Fellowship Research Reports. July 1934, Oct. 1936 and Jan. 1944. Chemistry of Portland Cement, R. H. Bogue, Reinhold Publ. Corp., p. 698, 1955.
4. Schwiete, H. E., and Niel, E. M. G. Formation of Ettringite Immediately After Gaging of a Portland Cement. Jour. Am. Ceramic Soc., Vol. 48, No. 1, pp. 12-14, 1965.
5. Kantro, D. L., Copeland, L. E., and Anderson, E. R. An X-Ray Diffraction Investigation of Hydrated Portland Cement Pastes. American Society for Testing and Materials, Proceedings, Vol. 60, pp. 1020-1035, 1960.
6. Chatterji, S., and Jeffery, J. W. Studies of Early Ages of Paste Hydration of Cement Compounds. Jour. Am. Ceramic Soc., Vol. 45, No. 11, 1962.
7. D'Ans, J., and Erick, H. The System $\text{CaO-Al}_2\text{O}_3\text{-CaSO}_4\text{-H}_2\text{O}$ at 20° C. Zement-Kalk-Gips, Vol. 6, pp. 302-311, 1953.
8. Turriziani, R., Schippa, G. The Chemistry of Cements. H. F. W. Taylor Ed., Academic Press, Vol. 1, Ch. 6, p. 263, 1965.
9. Carlson, E. T., and Bates, P. H. Engineering News-Record, Vol. 107, p. 130, 1931.
10. ASTM Standards for Cement, Lime and Gypsum, Part 9, p. 158, 1964.
11. Von Euw, M. Silicate Industry. Vol. 23, p. 647, 1958.
12. Locher, F. W. Solid Solution of Alumina and Magnesia in Tricalcium Silicate. Proc. Fourth International Symposium on Chemistry of Cement, NBS Monograph 43, p. 99, 1962.
13. Lea, F. M. The Chemistry of Cement and Concrete. Arnold Publishers, London, p. 206, 1965.
14. Carlson, E. T. Action of Water on Calcium Aluminoferrites. Jour. Res. NBS, Vol. 68A, No. 5, pp. 453-463, 1964.
15. Greene, K. T. Early Hydration Reactions of Portland Cement. Proc. Fourth International Symposium on Chemistry of Cement, NBS Monograph 43, pp. 328-366, 1963.
16. Bogue, R. H., and Lerch, W. Ind. Eng. Chem., Vol. 26, p. 837, 1934.
17. Seligmann, P., and Greening, N. R. Studies of Early Hydration Reactions of Portland Cement by X-Ray Diffraction. Highway Research Record 62, pp. 80-105, 1964.
18. Turriziani, R. The Chemistry of Cements. H. F. W. Taylor, Ed., Academic Press, Vol. 1, p. 278, 1964.
19. Chatterji, S., and Jeffery, J. W. Studies of Early Stages of Paste Hydration of Different Types of Portland Cements. Jour. Am. Ceramic Soc., Vol. 46, No. 6, pp. 268-273, 1963.
20. Kalousek, G. L. Analyzing SO_3 -Bearing Phases in Hydrating Cements. Materials Research and Standards, Vol. 5, No. 6, pp. 292-304, 1965.
21. Schwiete H., and Iwai, T. Behavior of Ferrite Phase During Cement Hydration. Zement-Kalk-Gips, Vol. 17, No. 9, pp. 379-386, 1964.